

**Drew University**

**College of Liberal Arts**

**Synthesis of Organic Compounds  
to Model Biological Systems**

**A Thesis in Chemistry**

**By: Delmis Hernandez**

**Submitted in partial fulfillment  
Of the Requirements  
For the degree of  
Bachelor in Arts  
With Specialized Honors in Chemistry**

**May 2016**

**Acknowledgements & Dedications:**

I would like to thank Dr. Keyser for being my research advisor during my junior year and working with her made me realize how much passion I have towards organic synthesis projects. I would also like to thank Dr. Cassano for being my research advisor during my senior year and allowing me to continue doing organic synthesis. I would like to thank Dr. Ronald Doll for collaborating with Dr. Cassano, guiding me and allowing me to work with him during this synthesis project. I would like to thank my Honors Thesis Committee, Dr. Dunaway and Dr. McGuinn, for helping me during the process of writing my thesis. Finally I would like to thank my family who has been very understanding during the process of writing my thesis.

**Abstract:**

Biological systems are composed of large macro-molecules that are responsible for the regulatory functions in the cell. These systems are important in order to learn about how the cell works and how it repairs itself. Additionally, these macromolecules are often used in industrial applications. Some of the research done on biological systems uses small molecules to study these macro-molecules. Small organic molecules can be synthesized and used to mimic the biological system of interest to learn about its stability, or its mechanistic pathway as well as other important aspects.

Surface salt bridge interactions are non-covalent interactions that are formed between two oppositely charged residues. The strength of surface salt bridges are still contentious regarding their contributions to the stability of a protein. During the course of this project, we sought to synthesize a biphenyl derivative, which mimics a solvent exposed salt bridge interaction, to measure the strength of this type of interaction present in protein. 2-Bromoxylene-m-xylene was converted to a diacid, then to a diester, then to a monoacid. 3-Hydroxypropionitrile was oxidized and then the addition of a protecting group was added to the alcohol. Once the final target molecule is isolated, the strength of the surface salt bridge interaction will be measured using NMR.

Another project where a small molecule approach may be helpful is in phosphorodithioates. Phosphorodithioates are modified oligonucleotides that are used to study phosphodiester cleavage. Phosphodiester cleavage happens relatively slowly, but can be catalyzed by a divalent metal ion. The mechanism for phosphodiester cleavage, and in particular the mechanism of metal-ion catalysis, is still the subject of much

investigation. In this project, we sought to synthesize 5'Uridine 3' Guanidine phosphorodithioate dinucleotide, (UPS<sub>2</sub>G), in order to use this molecule for kinetic studies and determine the role of metal ions in phosphodiester cleavage. The compound that has been successfully synthesized thus far is the phosphorothioamidite intermediate, with a 75.22 % crude yield. An automated solid synthesizer, which would usually be used for such a synthesis was not available and thus a modified strategy was developed using a centrifuge tube. Once the phosphorodithioate dinucleotide has been synthesized, the Cassano lab will use this molecule to study whether phosphodiester cleavage occurs at the same rate as the –oxo analogue.

## **Table of Contents:**

<b>Introduction</b>	<b>1-24</b>
Biological Systems	1-2
Salt Bridges	2-16
The Biological Question	2-14
The Small Molecule Approach	14-16
Phosphorodithioates	16-24
The Biological Problem	16-19
Phosphoro-monothioates & dithioates	19-23
The Chemical Solution	24-25
<b>Materials &amp; Methods:</b>	<b>25-36</b>
Instrumentation	25-30
NMR	25-27
TLC	27-29
HPLC	29-30
Synthesis	30-36
Salt Bridge	30-32
Phosphorodithioate	32-36
HPLC studies	36
<b>Results and Discussion</b>	<b>36-57</b>
Salt Bridge	36-46
Phosphorodithioate	47-57
<b>Conclusion:</b>	<b>58-65</b>
Salt Bridge	58-61
Phosphorodithioate	61-65
<b>References</b>	<b>64-69</b>

**Table of Figures:**

	<b>Page #</b>
<b>Figure 1.</b> Non-covalent interactions	3
<b>Figure 2.</b> Charged residues at physiological pH	4
<b>Figure 3.</b> Salt bridge interaction.	4
<b>Figure 4.</b> Factors contributing to stability of a salt bridge	6
<b>Figure 5.</b> Salt bridge interaction distance	6
<b>Figure 6.</b> A buried salt bridge and a surface salt bridge interaction	9
<b>Figure 7.</b> Target Molecule A	16
<b>Figure 8.</b> DNA dinucleotide	17
<b>Figure 9.</b> Dinucleotide with a phosphodiester bond	18
<b>Figure 10.</b> Phosphodiester bond cleavage as a 1-step mechanism	19
<b>Figure 11.</b> Phosphorothioate and phosphorodithioate dinucleotide	20
<b>Figure 12.</b> RNA intramolecular cleavage	21
<b>Figure 13.</b> Phosphorothioate interaction with a calcium ion	23
<b>Figure 14.</b> Target molecule I	24
<b>Figure 15.</b> NMR splitting of energy levels for a nuclei	26
<b>Figure 16.</b> General synthetic pathway to obtain target molecule A	38
<b>Figure 17.</b> <sup>1</sup> H NMR spectra of compound C	40
<b>Figure 18.</b> <sup>1</sup> H NMR spectra of compound D	41
<b>Figure 19.</b> <sup>1</sup> H NMR spectra of crude product compound E	43
<b>Figure 20.</b> TLC plate of the crude product E	44
<b>Figure 21.</b> <sup>1</sup> H NMR spectra of the crude compound G	45
<b>Figure 22.</b> TLC plate of compound H	46
<b>Figure 23.</b> General synthetic pathway to obtain target molecule I	48
<b>Figure 24.</b> <sup>1</sup> H NMR of J, K and literature NMR of K	50
<b>Figure 25.</b> ChemBio Results <sup>1</sup> H NMR of J	52
<b>Figure 26.</b> ChemBio Results <sup>1</sup> H NMR of K	52
<b>Figure 27.</b> Phosphorous NMR & Literature NMR of K	53
<b>Figure 28.</b> HPLC chromatogram of product mixture & guanosine	55
<b>Figure 29.</b> HPLC chromatogram of base hydrolysis study	56
<b>Figure 30.</b> HPLC chromatogram of guanosine, dinucleotide & product	57
<b>Figure 31.</b> Progress on the salt bridge project	60
<b>Figure 32.</b> Progress on the phosphorodithioate synthesis project.	63

## Table of Abbreviations

Boc: tert butyloxy carbonyl

RNA: Ribonucleic acid

$k_c$ : coulomb's constant

$q_1$ : charge on species 1

D: Dielectric constant

Å: Angstroms

DNA: Deoxyribonucleic acid

NMR: Nuclear Magnetic Resonance Spectroscopy

FT: Fourier Transform

I: Nuclear Spin

$\gamma$ : Magnetogyric ratio

B: Magnetic Field

h: Planck's constant

HPLC: High Performance Liquid Chromatography

TCA: trichloroacetic acid

NMP: N-methylpyrrolidinone

DDTT: (*E*)-5-(2-(dimethylamino)vinyl)-3*H*-1,2,4-dithiazole-3-thione

ACN: acetonitrile

DCM: dichloromethane

BuOH: butanol

MeOH: methanol

ppm: parts per million

UPS<sub>2</sub>G: 5'Uridine 3' Guanidine phosphorodithioate dinucleotide

NMR data abbreviations:

s: singlet

d: doublet

dd: doublet of doublets

t: triplet

**Introduction:****Biological Systems:**

Biological systems are important to study in order to gain insight on the mechanistic pathways that these systems employ. Biological systems are composed of large macromolecules a few examples of these systems are proteins and nucleic acids. Macromolecules are usually studied by mutagenesis studies. Mutagenesis studies done on proteins consist of the deletion or alteration of a gene, but this can cause more than the intended change in the resulting protein. For example, a mutation on a gene to study the effect a specific interaction has on the structure can alter multiple interactions in the vicinity of this mutation resulting in several effects, which are difficult to differentiate.<sup>1</sup> This can make mutagenesis a difficult method to use when studying biological systems and attempting to see a cause and effect with certain interactions.

In some cases, small molecules may be useful because it is easier to make mutations on the molecule and observe the effect these changes cause more directly. Small organic molecules usually mimic a specific portion of a macromolecule. The main goal of small organic molecules is to help understand a more complex biological system. This allows for the study of specific interactions in biological systems because this newly synthesized organic molecule can mimic this interaction.

In this research, in order to gain insight into specific interactions present in these complex biological systems, we will model them using their key characteristic building blocks. In this study, small organic molecules are synthesized so they can be used to study biological systems and learn their effect on function in varying conditions. This



study focuses on the syntheses of small molecules that act as models for surface salt bridge interactions and catalytic ribonucleic acids (RNA).

## **SALT BRIDGES:**

### **The Biological Question:**

Proteins are important to study because they determine the function of a cell. Proteins are made up of amino acids linked together, which is the primary structure of a protein. The primary structure determines the tertiary structure of the protein and in turn determines the function of the protein.<sup>2</sup> Proteins can function as catalysts, transport units, and have many other functions.<sup>2</sup> The interactions and structure of proteins are what determines their function in the cell. Non-covalent interactions are important because they are present in proteins and are factors that contribute to the overall structure and stability of the functional structure.

Proteins are used in industrial settings where they are used in detergents, bio devices and are the targets of many therapeutic drugs. Identification of the interactions present in a protein can help alter its stability and makes it easier for protein engineering.<sup>3</sup> Protein engineering can benefit from increasing the stability of a protein, an example is in bio devices. Bio devices are placed in harsh conditions, proteins cannot withstand harsh conditions; they will denature, so if this interaction can be further stabilized these devices will be able to withstand harsher conditions for longer periods of time.<sup>4</sup>

Intermolecular forces hold the three-dimensional structure of a protein together.<sup>2</sup> There are many different types of intermolecular interactions such as London dispersion forces, dipole-dipole interactions, and hydrogen bonds (Figure 1). London dispersion

forces occur in every molecule and are a result of induced dipoles that cause an attraction between the negative and positive ends of a molecule.<sup>5</sup> Dipole-dipole interactions are attractions between polar molecules with permanent dipoles. In dipole-dipole interactions the partially negative end of a molecule is attracted to the partially positive end of a molecule. Hydrogen bonds result attraction of a hydrogen atom attached to another oxygen, nitrogen, or fluorine to an electronegative atom.<sup>5</sup>

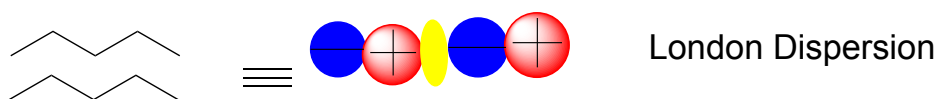


**Figure 1.** The different types of non-covalent interactions that are incorporated into a salt bridge interaction.

A salt bridge is a type of non-covalent interaction present in proteins; it is found in about 60% of proteins and is an important interaction that can contribute to the stabilization or destabilization of a protein.<sup>6</sup> An important interaction contributing to stability of a protein is a salt bridge interaction. Salt bridges are formed between negatively, and positively charged residues, such as glutamate and lysine respectively (Figure 2).<sup>7</sup> The salt bridge interaction also occurs with either the carboxylate terminus

(negatively charged) or the ammonium terminus (positively charged) at physiological pH (Figure 3).

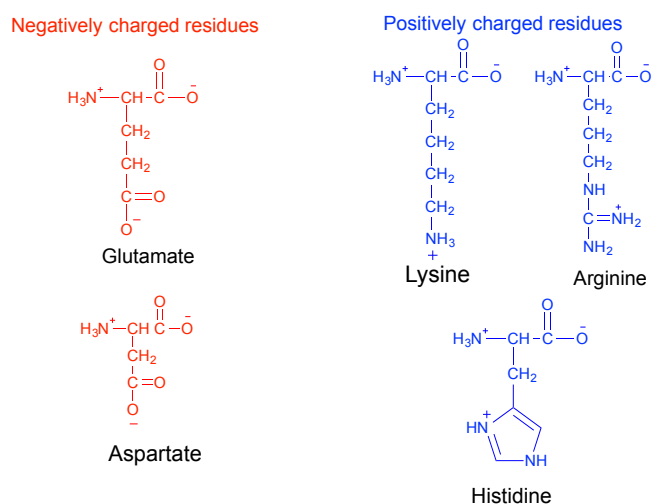


**Figure 2.** Five charged residues at physiological pH so have the possibility of forming a salt bridge with the side chain groups.

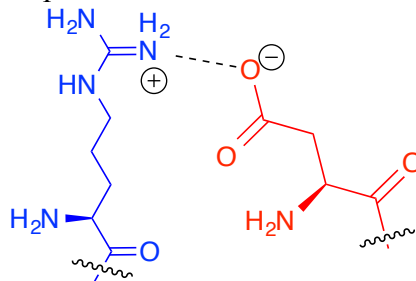


**Figure 3.** A salt bridge interaction between a positively charged residue and a negatively charged residue. This type of interaction can also be called a hydrogen bond.

A salt bridge interaction is pH dependent because salt bridges require oppositely charged residues. At physiological pH, carboxylic acids like glutamate and aspartate are negatively charged, while the ammonium terminus like lysine, arginine or histidine is positively charged (Figure 2). When conditions are acidic, the negatively charged residue becomes protonated and neutral, thereby lacking the ability to form a salt bridge. Similarly, at basic pH values, the positively charged residue of a salt bridge is

deprotonated and neutral. Thus, basic or acidic conditions do not favor salt bridge formation.<sup>8</sup>

Although salt bridges are generally thought to stabilize protein structure, their overall stability is attributed to a number of factors. The net contribution to stability arises from energetically favorable coulombic attractions, unfavorable desolvation energies and conformational constraints (Figure 4).<sup>8</sup> The favorable coulombic attraction is the attraction between a positive and negative charge. This attraction is easy to calculate using Coulomb's law. Equation 1 below shows Coulomb's law where  $k_c$  is coulomb's constant,  $q_1$  and  $q_2$  are the charge on the two residues,  $r$  is the distance between the two charges usually referred to as the charge separation distance and  $D$  is the dielectric constant, which is a measure of the polarizability of the solvent (Equation 1). The unfavorable desolvation energies must be low or insignificant in order for the interaction to be favorable. In desolvation, favorable interactions with the solvent are competing with the residues and the two residues must have a stronger attraction for them to interact and form a salt bridge. Conformational constraints, also called background, play a role and this has to do with the spatial arrangement of the two residues in order to form this interaction. The usual distance between residues has been speculated to be about 4 Å (Figure 5).<sup>8</sup>

$$F = k_c \left( \frac{q_1 q_2}{Dr^2} \right) \text{ Equation 1.}$$

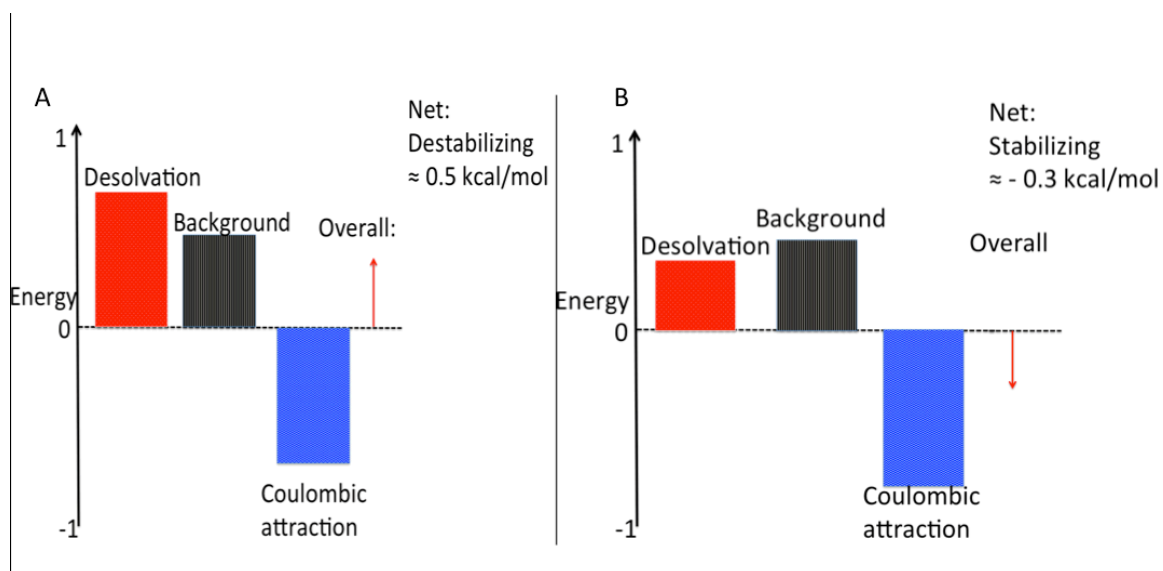


**Figure 4.** A) Displays an overall favorable salt bridge and B) displays an overall unfavorable salt bridge determined by three factors, desolvation, conformational constraint (background) and coulombic attraction.

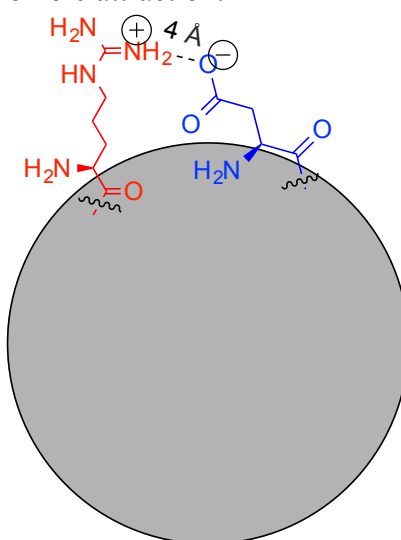


**Figure 5.** A salt bridge interaction in a protein. The usual distance between two residues when forming a salt bridge interaction is usually about 4 Å.

Salt bridges are present in over 60% of proteins.<sup>6</sup> This non-covalent interaction can exist in two forms, a buried salt bridge and a surface salt bridge. A buried salt bridge refers to salt bridges found deep in the protein. A buried salt bridge can occur as either stabilizing or destabilizing. The cost of burying a charged residue in the center of a

protein can actually be high which is why the contribution to stability that the interaction provides can be low or it can make the interaction destabilizing. Although this is true, the reason why buried salt bridges tend to be stabilizing is because this interaction is enthalpically favorable since it has no other potential bonding partners. The dielectric in the interior of a protein is low thus the coulombic attraction is high.

It was found that a single buried salt bridge, in the hydrophobic core of a molecule stabilized a T4 lysozyme by more than 5 kcal/mol.<sup>9</sup> The stabilizing force of buried salt bridges lies in the interior of the protein when it establishes ionic interactions with other polar groups. Additionally, in the interior of the protein there is a low desolvation penalty associated because there is no solvent found in the interior of the protein that could interact with the attracting residues.<sup>10</sup> In another study, researchers found that halophilic proteins, proteins that thrive in salt rich environments, have buried salt bridges and the majority of these buried salt bridges are stabilizing.<sup>11</sup> Researchers studied 275 salt bridges from 20 different halophilic proteins; this protein has a higher proportion of buried salt bridges. Their main finding was that 80 % of the salt bridges contributed to stability of the protein.<sup>11</sup>

However, buried or partially buried salt bridges have also been found to be destabilizing to the protein structure. It was found that 19 % of the buried salt bridges studies were unstable.<sup>11</sup> The cost of burying a charged residue in the center of a protein is high due to the energy needed to desolvate the residues which is why the contribution to stability can be low. It is unknown when exactly a buried salt bridge is stabilizing or

destabilizing. However, a small molecule can help determine what factors contribute to the strength of the interaction.

Buried salt bridges are important to study in order to understand the stability and folding pathways of proteins. Buried salt bridges are interactions that can affect the protein. It was found that buried salt bridges can modulate the allosteric behavior of the protein since the buried salt bridge can act as a binding site in an enzyme.<sup>10</sup> Allosteric behavior is when a substrate binds somewhere other than the active site, but causes the active site to change.

A buried salt bridge and a surface salt bridge interaction are different due to the environment that surrounds them (Figure 6). A surface salt bridge is exposed to solvent and this interaction may not be as stabilizing as buried salt bridges because the linking residues can interact preferentially with the solvent.<sup>3</sup> Surface salt bridges are formed on the surface of proteins, usually in the presence of solvent. Charged residues are very commonly found on the surface due to their ability to form interactions with the solvent.<sup>12</sup> Residues present on the surface of proteins can form a salt bridge interaction, but the solvent can form a competing ion-dipole with the residue, thereby breaking the salt bridge.<sup>12</sup> Salt bridge interactions are highly important because they can affect the protein structure. There is evidence from previous studies that demonstrate that the disruption of surface salt bridges can lead to protein compaction, a tighter protein structure where interactions are now closer to each other.<sup>13</sup> Creating or destroying salt bridge interactions alters the interactions found in a protein, which can affect the folding of the protein.

Salt bridges with favorable geometries can be stabilizing regardless if they are on the surface or buried in the protein if the energy is high enough to overcome other factors that make the salt bridge destabilizing.<sup>14</sup> Surface salt bridges present in thermophilic enzymes are generally stabilizing, because these proteins live in areas of high temperatures and there is a reduced desolvation penalty at high temperatures.<sup>14</sup> At higher temperatures, water is removed more easily. Additionally, many thermophiles have an increased number of salt bridges that exist within a network of salt bridges, which cooperatively and mutually strengthen each other; the interaction is therefore stronger than if it were isolated.<sup>16</sup> Research on salt bridges focuses a lot on determining when the salt bridges are stabilizing or destabilizing and how it affects the protein.

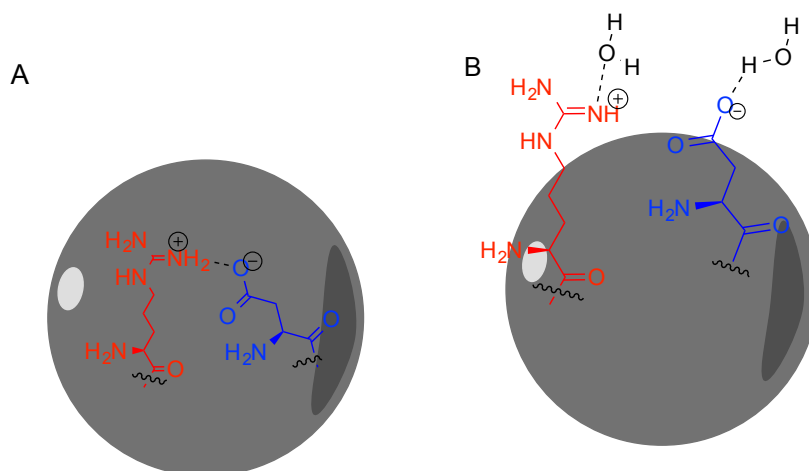


**Figure 6.** A) Buried salt bridge and B) A surface salt bridge interaction that is not formed. The surface salt bridge is not formed because the residues are interacting with the solvent rather than with an oppositely charged residue.

Previously, researchers used histone like HU proteins, the protein with the mutation, Hbsu-D26A experienced an enhancement in DNA compaction.<sup>15</sup> Researchers concluded that the formation of a salt bridge occurred, and some of the salt bridges were forming with DNA phosphates. The disruption of salt bridges has also been observed



when the salt concentration is increased because the thermodynamics of binding decrease with increasing salt concentration.<sup>15</sup> This is an interesting finding because in a particular study, it was found that when the concentration of potassium ions increased so did the tendency to form direct or indirect salt bridges.<sup>16</sup> Some salt bridges are disrupted in the presence of salt because when researchers studied HU proteins they added cations that caused an interaction with the negatively charged residues and thus the positively charged residues can now only interact with solvent.<sup>15</sup> In this one particular case though, salt bridges can form when there is an increase in cation concentration yielding more salt bridges because the presence of the cations increases the helicity, the protein becomes more coiled, and can bring two oppositely charged residues closer together and farther from solvent increasing the probability of a salt bridge forming.<sup>16</sup> The exact effect salt has on the energy of a salt bridge is unknown, but a small molecule system can help determine the role of salt ions.

It was found that if there are two salt bridges present in a protein the interactions could demonstrate different degrees of stability, meaning that not all salt bridges contribute equally to stability. Strop *et al.* studied proteins from thermophilic organisms and examined whether salt bridges stabilize the protein rubredoxin.<sup>17</sup> Researchers concluded that the side chain to side chain salt bridge between lysine 6 and glutamate 49 in rubredoxin did not contribute to protein stability. On the other hand, another salt bridge found in this protein, between a main chain residue, on the backbone, and side chain residue, contributed to stability of the protein.<sup>17</sup> The main reason is because the salt bridge between lysine 6 and glutamate 49 had to be desolvated and immobilized, the

residues had to lose degrees of freedom to form the interaction. Meanwhile the other salt bridge has a smaller penalty for immobilization since a residue is on the backbone and thus not mobile.<sup>17</sup>

There is no correlation between an increase in the possible number of salt bridges and protein stability. Sokalingam *et al.* studied the effect of changing lysine residues to arginine residues to enhance the stability of green fluorescent protein (GFP) (Figure 2).<sup>18</sup> This mutation was conducted due to arginine's superior ability to chelate in a bidentate fashion, so theoretically it would form two salt bridges instead of one by just mutating a residue. Initially researchers mutated all 19 lysine residues to arginine but observed no improvement in stability, which indicated that the lysine residues were vital to protein folding. They then mutated 14 lysine residues and tested the stability of this new mutated protein, GFP14R against GFPcon, the protein with no mutations. The mutant, GFP14R, showed stability in up to 5 M urea and showed activity loss at 6 M urea. The mutant protein began to show higher stability than GFPcon at basic pH values. GFP14R had 5 new salt bridges and 9 new hydrogen bonds; researchers concluded that the new arginine residues that led to the formation of new salt bridges and hydrogen bonds on the protein's surface, enhancing the stability of the protein when placed in harsher conditions.<sup>18</sup>

Meuzelaar *et al.* also concluded that the net free energy contribution of a salt bridge could range from highly stabilizing to highly destabilizing.<sup>19</sup> They investigated the arc repressor of bacteriophage P22 and the effect glutamate-arginine salt bridges had on the kinetics of folding and unfolding of  $\alpha$ -helical peptides. Researchers found that salt bridges destabilize the native state of the protein and that a salt bridge could possibly

slow down or speed up the folding rate of a protein depending on the geometric orientation and distance between the interacting residues.<sup>19</sup>

Researchers investigated a specific salt bridge that was located in the protein L9. The residues involved in this interaction were aspartate 23 and the protonated N-terminus of the main chain, the amino end of a residue.<sup>20</sup> This salt bridge was studied using a double-mutant analysis. Mutations modified the residue aspartate to an alanine, asparagine, and to an alanine with a nitrile. The main finding was that the coupling free energy was large and favorable and the main chain salt bridge had a favorable -1.5 kcal/mol interaction energy.<sup>20</sup> The stability or instability of a salt bridge varies from protein to protein, but it is known that the environment surrounding the salt bridge is what affects the interaction.

Phelan *et al.* also concluded that salt bridges do not stabilize all protein structures.<sup>8</sup> They found that the protein was mainly stable at pH values between 2-8 since salt bridge formation is not favorable at either acidic or basic pH values. Computational analysis of the leucine zipper revealed wide variations in the energetics of interhelical ion pairs. Removing charged residues by mutation destabilized the coiled coil by 0.23-0.47 kcal/mol per residue; this was attributed to the loss of salt bridges because as you remove a charged residue, a salt bridge is being removed.<sup>8</sup>

Although some research suggests that salt bridges may be stabilizing to a protein structure, this may not be the case because it may be more favorable for the residue to interact with solvent. Energetically favorable coulombic interactions between residues are often counteracted by entropy loss. There is a loss in entropy since the degrees of

freedom of a residue are lost when participating in an interaction. Additionally, coulombic attractions can also be counteracted by the unfavorable desolvation cost. In the quantification of salt bridge strength, researchers have relied upon either computational or mutagenesis studies. Computational studies have been inconclusive in determining the strength of salt bridges. Mutagenesis studies have been difficult since they can cause changes in protein structure. The new advances in computer hardware and software have extended the time scales that biomolecular simulations can be ran for, which is essential for evaluations of biomolecular force fields.<sup>21</sup> Computer simulations can also determine the strength of salt bridges as a function of temperature, thermodynamics, and kinetics of dimerization.<sup>22</sup>

Many experimenters use molecular dynamic (MD) simulations to determine what is the rate-limiting step, or the slow step in the formation of a salt bridge. In one such experiment it was found that the rate limiting step was the rate of breaking a solvent exposed salt bridge.<sup>22</sup> Computer simulations have an advantage over other methods; testing of different molecules in a short amount of time can be done using computer simulations, and saves money as there is no need to purchase new materials for the investigation of different proteins. The disadvantage is that sometimes you can have an interaction occur according to computer simulations, but the interaction might not actually occur if it is more favorable for the molecule to interact with something else.<sup>22</sup> In computer simulations, a thorough understanding of the system is needed in order to obtain accurate results. If the subject of investigation is not known very well, the likely interactions that it may participate in will not be the actual results obtained from the

simulations.

Mutagenesis studies is another useful method to study salt bridges.<sup>22</sup> Mutagenesis is when there is a mutation of certain residues; then a comparison between the wild-type protein, the protein with no mutation, and the mutant protein is done. The disadvantage is that mutagenesis can cause a change in protein structure and thus other interaction are changed, making it difficult to draw a concrete conclusion from this type of data.<sup>22</sup>

Hunter's cycle also called double mutant cycles (DMC) is yet another approach of studying salt bridge interactions. Double mutant cycles are used to study weak non-covalent interactions present in proteins.<sup>23</sup> The way DMCs work is that for the interaction of interest, both residues participating in the interaction are singly mutated.<sup>24</sup> For DMCs to work effectively the mutations should not cause a change in protein structure or the results are useless. The disadvantage to this method is that it cannot be an important interaction present in the protein. An important interaction will alter the structure of the protein dramatically making DMCs inappropriate. Also, when studying salt bridges the accuracy of these measurements diminishes because of experimental error.<sup>24</sup> This method can also only be applied to large systems and not small ones or synthesized ones.<sup>23</sup> Experimental data is needed and a small molecule model where the environment can be altered can help determine how much each factor contributes to the overall strength of a salt bridge interaction.

### **The Small Molecule Chemical Approach:**

There are many different ways that salt bridges may be studied in order to determine their net effect on protein structure. Here, a small molecule is used to study a

solvent-exposed salt bridge interaction. Small molecules are helpful when studying biological systems because the small molecule can mimic a particular interaction in a large system and any mutations done on the small molecule will not cause a global change in the structure of the molecule. The small molecule approach makes it easier to draw conclusions from the data obtained.

In a study, scientists wanted to learn about the mechanism of phosphoryl transfer in phosphatases.<sup>25</sup> In order to study this large enzyme, they synthesized a small molecule that would mimic the active site of the phosphatase. The use of the small molecule allows them to study this enzyme's active site without doing mutations that could possibly change the structure of the enzyme. The interactions in small molecules are easier to manipulate than the ones in macromolecules.

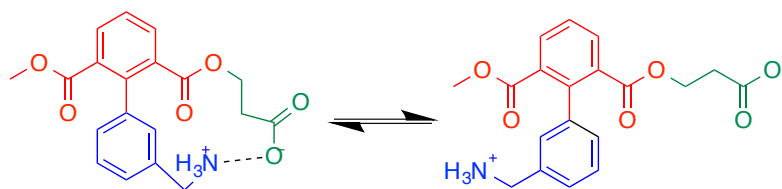
In our study, a small molecule will help determine the contribution a salt bridge interaction has on protein stability. The use of a small molecule will enable us to study a single interaction and draw conclusions from it. This is important because in a protein structure affecting one interaction can cause more interactions to change, making it difficult to draw clear conclusions from the data.

In our research, we seek to determine if a solvent-exposed salt bridge will form and if so, determine the strength. The residues can interact preferentially with the solvent causing no salt bridge formation. The goal is to synthesize a small molecule, which has the potential of forming a solvent-exposed salt bridge interaction. Once the synthesis of this compound is complete, this interaction will be used to measure the strength of the interaction.

The synthesis of a small molecule, which has the possibility of forming a solvent exposed salt bridge interaction, was attempted. Our model of a surface salt bridge interaction will be achieved by the synthesis of a biphenyl molecule (Figure 7). Our model system has two different conformations; one forms a salt bridge interaction while the other does not. Additionally, this model system allows us to determine the strength of a solvent-exposed salt bridges in varying solvents. This enables us to understand how the desolvation cost differs depending on the solvent and whether certain solvents tend to form more stable salt bridges. This model system can also help determine the effect salt concentration, temperature of varying pH values have on the salt bridge interaction.

Once the synthesis of this compound is complete, the strength of the salt bridge will be quantified under many conditions modeling protein environments. The strength of the interaction can be quantified by determining the ratio of the two conformers of this molecule from the  $^1\text{H}$  NMR spectrum. Then a  $K_{eq}$  value can be calculated and used to determine the  $\Delta G$  value for this surface salt bridge interaction (Equation 2). The salt bridge that will be synthesized will help elucidate what factors contribute in making this interaction a stabilizing force (Figure 7).

$$\Delta G^\circ = -RT \ln(K_{eq}) \quad \text{Equation 2.}$$



Target Molecule, A

**Figure 7.** Molecule A, our desired target, will mimic a salt bridge interaction.

## PHOSPHORDITHIOATES:

### The Biological Problem:

Deoxyribonucleic acid (DNA) is the carrier of genetic information of species. DNA exists as a double helix, which runs in opposite directions. Each strand has a backbone where nucleotides are linked by a phosphodiester bond. The linkage occurs on the oxygen of the 3' carbon of one nucleotide and the oxygen on the 5' carbon of the other nucleotide unit (Figure 8). DNA is important as well as ribonucleic acid (RNA), these two are present in all life forms. The main structural difference between RNA and DNA is that RNA has a hydroxyl group on the 2' carbon. Genetic information is copied from DNA into RNA and then translated into a protein.<sup>26</sup> RNA is essential to life forms because it carries genetic information when it is transferred from DNA. Another form of RNA, are catalytic RNAs sometimes referred to as ribozymes.<sup>26</sup> Ribozymes play important roles in cellular functions such as RNA processing and their catalytic mechanisms involving metal ion cofactors have received intense study.

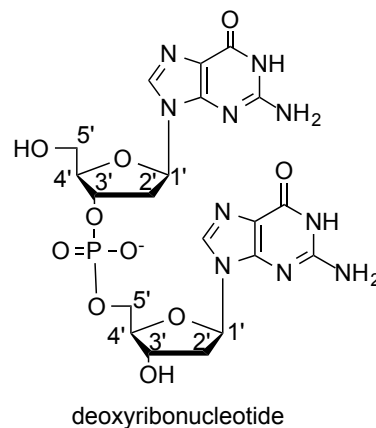


**Figure 8.** Two nucleotides long, deoxyribonucleotide, linked by the 3' and 5' oxygen. DNA molecules have no hydroxyl group on the 2' carbon.

Phosphodiester bonds are the bonds that link nucleotides together and thereby are



of vital importance in RNA and DNA. An oligonucleotide is a series of nucleotide bases linked together by phosphodiester linkages (Figure 9). Phosphodiester bonds consist of a phosphate group that has two bridging oxygens and two non-bridging oxygens. The bridging oxygens are what hold two or more nucleotide units together; it is a connection between the 3' oxygen of one nucleotide and the 5' oxygen of the other nucleotide.

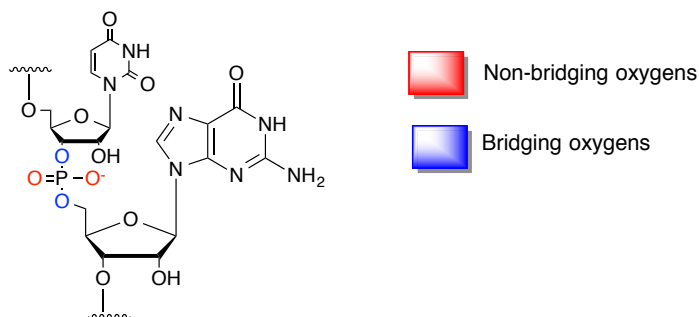


**Figure 9.** Two RNA nucleotides linked together by a phosphodiester bond, the curved lines indicate that there are more nucleotides linked. Linkage occurs from the 3' oxygen and the 5' oxygen. The bridging oxygens are highlighted in blue while the non-bridging oxygens are highlighted in red.

There are specific enzymes that can cleave phosphodiester bonds and they are called nucleases. Phosphodiester bond cleavage involves the attack of a nucleophile on the phosphorous center to break apart the nucleotide subunits.<sup>27</sup> The cleaving of these bonds is quite slow even though this is a favorable process.<sup>28</sup> The half-life of phosphodiester bond cleavage is around 30,000,000 years in physiological conditions.<sup>28</sup> Even though the half-life is so long, cleavage must occur at a relatively rapid pace to support life. Thus this reaction is catalyzed by divalent metal ions in a matter of seconds.

Phosphodiester cleavage occurs quickly when catalyzed by a divalent metal ion. Although the role of the divalent metal ion in the mechanistic pathway of phosphodiester cleavage is unknown, it is known that it is necessary in order for it to catalyze this

cleavage.<sup>28</sup> Phosphodiester bond cleavage is important for biological events. It is vital to discover the mechanism of this cleavage because revealing the mechanism can help in advances, such as deleting detrimental mutations. Many researchers focus on inhibiting the enzyme that cleaves nucleotide subunits in order to administer therapeutic agents and thus allowing these oligonucleotides to serve as drugs to remain active longer.<sup>29</sup> The way metal ion catalyzed phosphodiester cleavage is studied is by using phosphorothioates and comparing its cleavage rates to the –oxo analogue.

Researchers studied the cleavage of hepatitis delta virus in the presence of various different metal ions.<sup>30</sup> Evidence suggests that during HDV cleavage, the metal ions can stabilize the tertiary folding of HDV RNA, contributing to the catalysis of bond cleavage of RNA molecules.<sup>30</sup> In another study, researchers concluded that phosphodiester bond cleavage is catalyzed in two steps, very similar to a 1-step mechanism, where the nucleophile attacks, resulting in inversion of stereochemistry (Figure 10).<sup>29</sup> Using computational methods they determined that two divalent metal ions are present in the active site in order to catalyze phosphodiester cleavage.<sup>29</sup>

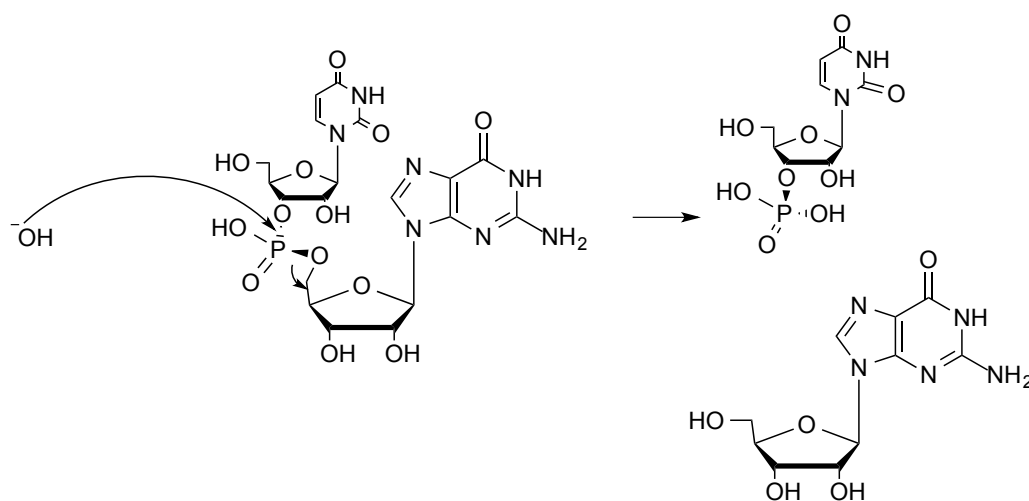


**Figure 10.** Nucleophilic attack resulting in inversion of stereochemistry.

### Phosphoro-monothioates & dithioates:

Oligonucleotides with modified phosphodiester bonds, such as phosphorothioates or phosphorodithioates are important because they are resistant to nucleases, meaning that nucleases cannot break these bonds.<sup>31</sup> Phosphorothioates are nucleotides that have only one non-bridging oxygen at the phosphodiester bond while the other non-bridging ligand is sulfur, while phosphorodithioates are characterized by the replacement of both non-bridging oxygens to sulfurs (Figure 11).

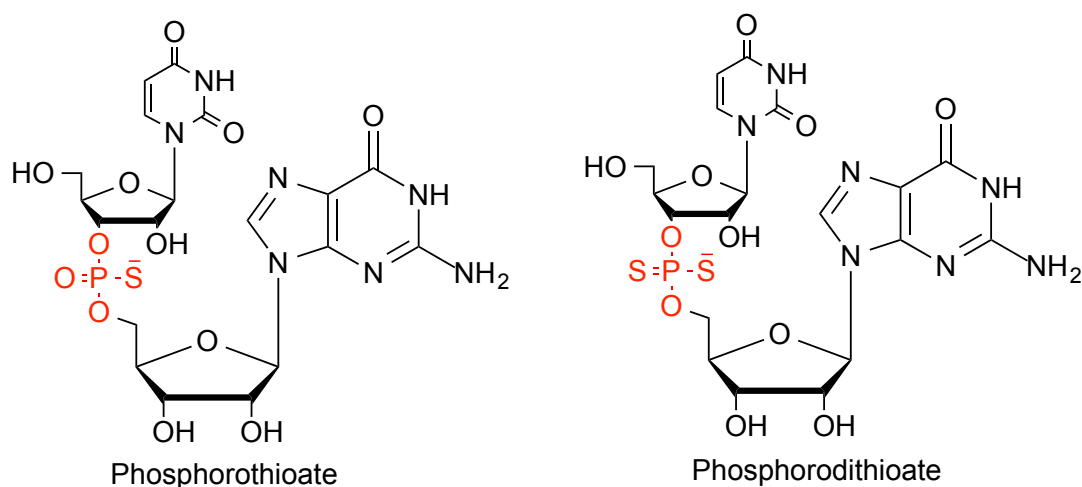


**Figure 11.** An example of a phosphorothioate and phosphorodithioate dinucleotide. The phosphodiester bond is highlighted in red.

Phosphorothioates and dithioates are also used to study the cleavage rates of phosphodiester bonds since cleavage happens at a slower rate.<sup>32</sup> These thioates can give insight into the mechanistic pathway of metal ion catalyzed phosphodiester bond cleavage. If thioates are resistant to nucleases because the divalent metal ions do not like interacting with sulfurs this means the cation is directly interacting with the non-bridging ligand. On the other hand, if the thioates have the same rate of cleavage as the oxo-

analogue then that means that the divalent metal ion do not directly coordinate with the ligand.

Phosphorothioates in the presence of magnesium can slow catalysis by 4 orders.<sup>32</sup> Magnesium does not interact as favorably with sulfur compared to oxygen, which explains the rate in change of this cleavage. Cleavage will occur more readily for RNA phosphorothioates than for DNA thioates since RNA molecules have an additional hydroxyl group at the 2' position which can act as a nucleophile and then sulfur is a better leaving group compared to oxygen (Figure 12).<sup>32</sup> This means there is an adjacent nucleophile to the modified center, which enhances the reactivity of the oligomer towards phosphodiester bond cleavage.<sup>32</sup> In our study, we focus on RNA molecules rather than DNA.

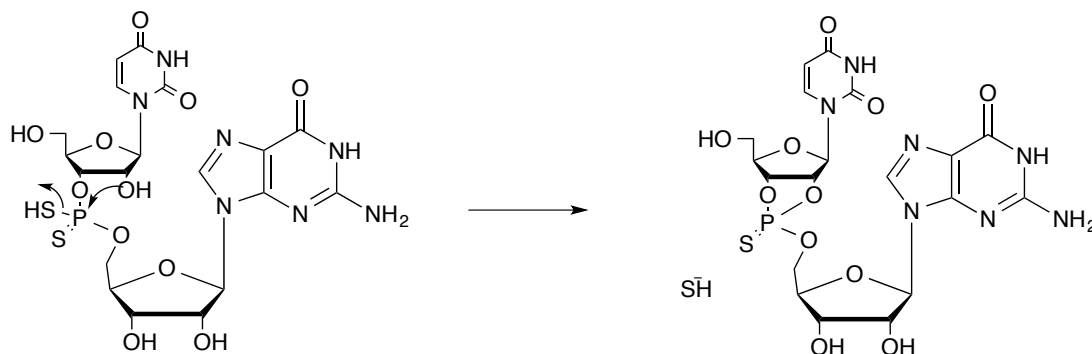


**Figure 12.** RNA's have a higher propensity to undergo cleavage due to the hydroxyl at the 2' position being able to act nucleophilic and the sulfur being a better leaving group compared to oxygen.

Researchers who study the cleavage rates of phosphorothioates or dithioates do so by varying divalent metal ions. It is known that soft metals, such as mercury (Hg) and silver (Ag) cause rapid cleavage of the bridging 3' and 5' phosphorothioates. The reason for increased rate of cleavage is due to soft vs. hard theory where hard acids interact with

hard bases more favorable and soft acids with soft bases. An atom is defined as hard when it is small and non-polarizable such as oxygen. Soft acids or bases are large polarizable groups, such as sulfur or mercury. Since sulfur is a soft base and mercury is a soft acid, this interaction would be more favorable than magnesium, a hard acid.

Direct metal ion coordination can be deduced from hydrolysis experiments,<sup>33</sup> in which a phosphorothioate bond is cleaved when thiophilic metal ions are used rather than non-thiophilic metal ions. Research conducted has led to the conclusion that soft metals, also called thiophilic metals, relieve some of the inhibition. When magnesium is replaced with manganese it was reported that ribozyme cleavage was relieved by a factor of 280.<sup>34</sup> Researchers here concluded that although magnesium still binds to the active site, the reason why it does not catalyze cleavage is because it is not able to stabilize the thio anion leaving group.<sup>34</sup>

Researchers are not even quite sure how many divalent metal ions are required for catalysis. Researchers hypothesize that phosphodiester bond cleavage occurs via the use of two metal ions.<sup>35</sup> The reason for their hypothesis of two or more metal ions being required is because the metal has to bind to binding sites as well as to the active site to catalyze this cleavage.<sup>35</sup> In another study, it was found that a single soft metal ion causes cleavage of phosphorothioates.<sup>36</sup> It is unclear how many and what exactly the metal ions are doing in phosphodiester cleavage. Thus, assays, which can more directly identify possible metal-ion coordination sites, are of great value.

One such experimental strategy is the metal-ion specificity switch. Previously, researchers studied the cleavage rate of a Ribonuclease P RNA which is a ribozyme.<sup>33</sup>

Two different RNA compounds were compared, an unmodified RNA and a modified RNA where one of the non-bridging oxygens is replaced by a sulfur. For the unmodified RNA, the cleavage rate under the conditions of 15 mM  $Mg^{2+}$  was  $3.3 \text{ min}^{-1}$ ; while for 15 mM  $Cd^{2+}$  it was less than  $10^{-4} \text{ min}^{-1}$ . For the modified RNA, cleavage was observed at  $3 \times 10^{-4}$  under 15 mM  $Mg^{2+}$  conditions and  $0.2 \text{ min}^{-1}$  at 15 mM  $Cd^{2+}$ . Cleavage was hindered for the modified RNA when the metal ion used was magnesium, but cleavage was relieved when the metal ion was cadmium. Thus, the change from an oxo species to a thio species and the change in metal ion was interpreted to indicate a direct-metal ion coordination.<sup>33</sup>

Previously, in the Cassano lab, the cleavage of a phosphorothioate dinucleotide was analyzed (Figure 13). The Cassano labs bought a phosphorothioate and examined whether the catalysis of this reaction was slowed down due to the replacement of a non-bridging oxygen with a sulfur. Their results indicated that catalysis was slowed down by at least 2 or 3 fold for the different diastereomers of this molecule, but catalysis was not hindered significantly. This means either cleavage is occurring by a different mechanism or the interaction of calcium with one of the non-bridging oxygens is enough for it to catalyze this cleavage. Another small molecule system where both non-bridging oxygens are transformed to sulfurs could help elucidate the role of metal-ions in phosphodiester bond cleavage.

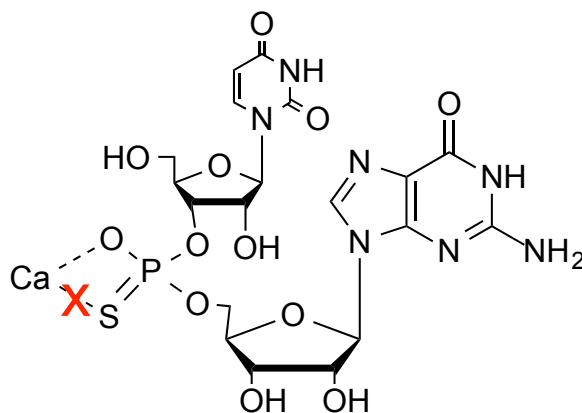


**Figure 13.** The calcium is not directly interacting with the non-bridging sulfur since this interaction is not favorable.

### Chemical Solution:

In our research, we sought to synthesize a phosphorodithioate dinucleotide in order to test the cleavage rate of this dinucleotide. Although there is an automated synthesizer that can do the chemistry to synthesize the dinucleotide, none were available for our use. Thus, a different synthetic strategy was developed. The reason why this dinucleotide is being synthesized is so the Cassano lab could perform kinetic studies on it (Figure 14). As mentioned earlier, the mechanism for metal-ion catalyzed phosphodiester cleavage is unknown. The synthesis of a phosphorodithioate dinucleotide, along with kinetic studies can help elucidate the role of metal ions in phosphodiester cleavage.

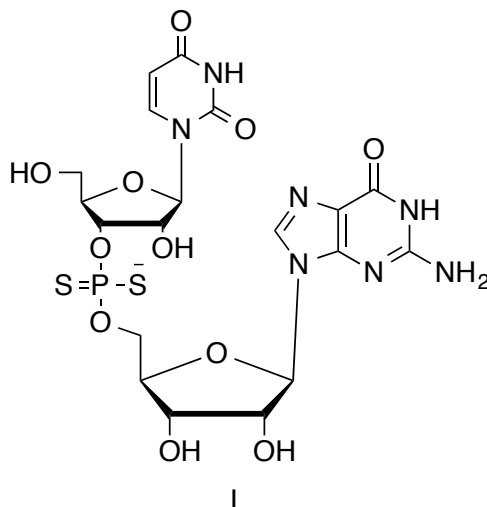


**Figure 14.** Target molecule I is the modified dinucleotide that will be used to do kinetic studies and determine the rate of cleavage.

The modified dinucleotide will help elucidate the mechanism of phosphodiester cleavage. If phosphodiester cleavage does go through an intermediate, a conclusion can be reached as to whether the negative charge formed is stabilized by a divalent metal ion. If the role of the metal ion is to stabilize the negative charge on the non-bridging oxygens then catalysis should be hindered significantly when a non-thiophilic divalent metal ion, such as calcium, is used. On the other hand, if catalysis is not hindered significantly, then the phosphodiester cleavage may be occurring through a different mechanism. Synthesis of this dithioate dinucleotide can help elucidate the mechanism of phosphodiester bond cleavage.

### **Experimental Section:**

#### **Instrumentation:**

#### **Nuclear Magnetic Resonance Spectroscopy (NMR):**

400 MHz Bruker NMR Spectrometer (FT-NMR Spectrometer):



NMR Spectroscopy is used for structural characterization. In NMR spectroscopy, nuclei will absorb electromagnetic radiation in the radio frequency. The radio frequency region which nuclei absorb is in the range of 4 to 900 MHz.<sup>37</sup> The atomic nuclei that have the property of spin are the ones with an odd mass number and any atomic number or even mass and odd atomic number. These atomic nuclei have a magnetic moment and thus when exposed to a magnetic field this leads to a splitting of energy levels (Figure 15).<sup>35</sup> NMR spectroscopy takes advantage of the fact that every atom has a nuclear spin of either 0,  $\frac{1}{2}$ ,  $1\frac{1}{2}$ , 2, etc. Table 1 below shows the nuclear spin properties associated with atoms of selected atomic mass and number.<sup>38</sup>

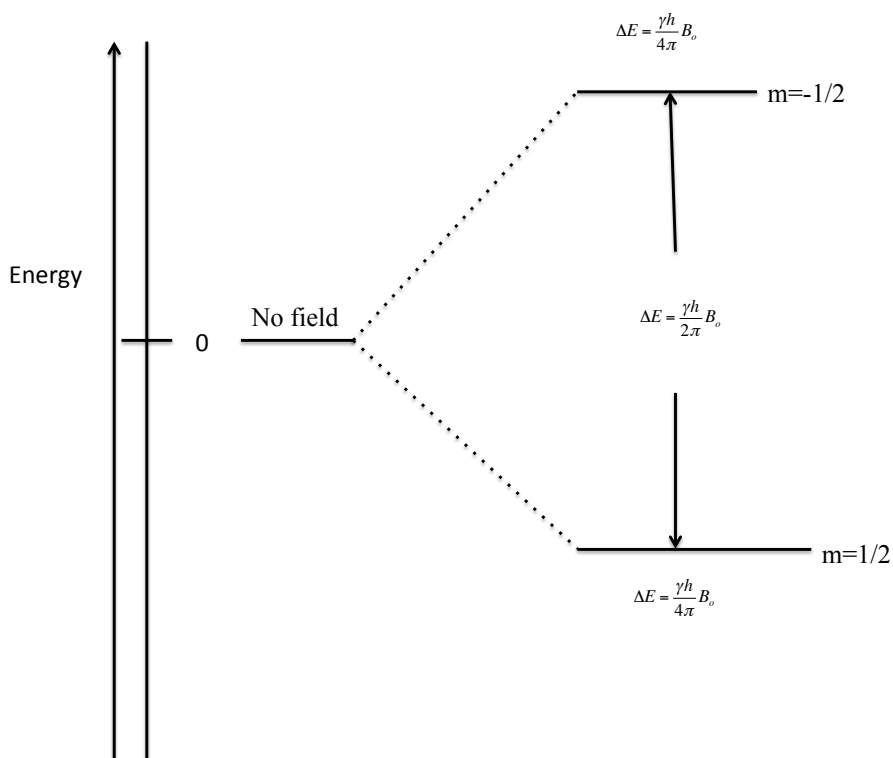


**Figure 15.** The splitting of energy levels for a nuclei with a spin quantum number of  $\frac{1}{2}$ .<sup>37</sup>

Mass Number	Atomic Number	Nuclear Spin
-------------	---------------	--------------

Odd	Even or Odd	$\frac{1}{2}, 1\frac{1}{2}, 2\frac{1}{2}$
Even	Even	0
Even	Odd	1, 2, 3

**Table 1.** The nuclear spin associated with an atom with a certain mass number and atomic number.

Any nuclei with an even mass number and even atomic number has a nuclear spin  $I=0$  which means it would have no NMR properties.<sup>37</sup> Nuclei with  $I = \frac{1}{2}$  are more suitable to be analyzed by NMR spectroscopy. When the nuclear spin is  $\frac{1}{2}$  there are two aspects one should consider. First, can the frequency of applied radiation or the magnetic field be varied. If so, then a signal can be obtained. If there is more than one atom it can interact with, any nuclei with the same spin, then this will cause a splitting pattern otherwise known as the  $2I+2$  or  $n+1$  rule.<sup>37</sup> Lastly, if the nuclei spin is 1 or greater, this means that the nuclei possess an electric quadrupole moment along with their magnetic moment property. The quadrupole moment interacts with the electric field and this produces an efficient way to relax the nuclei back down to ground state. This additional property can produce an NMR signal that is broadened.<sup>37</sup>

When an NMR signal is obtained, this affects the population of the spin state, fixed by relaxation time.<sup>38</sup> When there is no magnetic field present, the nuclei will present no energy difference in the energies of the magnetic quantum states because the nucleus is not absorbing electromagnetic radiation.<sup>38</sup>

The chemical shift and integration of a peak is used to determine the functional groups present in a molecule as well as the structure of the compound.<sup>37</sup> The exact chemical shift of certain compounds depends on the NMR solvent used.<sup>37</sup> A

magnetic field is applied, the electrons bonding the proton precessing the nucleus in a plane perpendicular to the applied field. This results in a secondary opposing field and thus the nucleus experiences a field that is smaller, so the nucleus is more shielded. The more shielded the more upfield the signal. There are NMR tables of where functional groups usually show up in NMR spectroscopy. Integration describes the number of protons associated with a certain compound. This allows for better structural characterization.

### **Thin Layer Chromatography (TLC):**

Thin Layer chromatography is a technique used to determine the different components found in a mixture.<sup>39</sup> A plate fused with silica gel is used, along with a chamber with the desired mobile phase. The plate is spotted with the reaction mixture; the reaction mixture should have UV active compounds in order for it to be seen. Once the plates have been spotted, they are placed in the chamber with the desired mobile phase. The solvent is allowed to travel and then removed from the sealed chamber. The different spots in the plate are marked, each different spot corresponds to the different component found in the mixture.<sup>39</sup>

The way each spot migrates up a TLC plate is not random, it depends on the mobile phase chosen.<sup>39</sup> If the mobile phase is more non-polar, the non-polar components will travel down the TLC plate faster than the polar components, which will either travel slower or remain near the baseline. The reason why they may remain near the baseline is because polar components can interact more with the stationary phase. The stationary phase on a TLC plate is silica gel, which is a silicon-oxygen repeating unit.

Each spot found on the TLC plate can be described by its retention factor (Rf) (Equation 3).<sup>39</sup>

$$Rf = \frac{\text{distance spot travelled}}{\text{Distance solvent travelled}} \text{ Equation 3.}$$

In this research project, TLC is used to characterize compounds synthesized. In order for the compounds to be seen on the TLC plate, they have to be UV active or aromatic compounds. The limitation to TLC characterization is that it will only tell you if you have UV active compound, and thus only certain compounds synthesized can be characterized using this method. TLC was used as an alternative method to characterizing compounds by NMR spectroscopy. In this research project, the mobile phase was 2:1 hexanes: ethyl acetate.

#### **High Performance Liquid Chromatography (HPLC):**

Liquid chromatography is a technique for analytical separation of different components in a solution. HPLC is a technique that operates at high pressures.<sup>39</sup> When a solution is injected into the column, a chromatogram is generated with peaks. The peaks in the chromatogram represent the different components/molecules in the solution that are separated because they have different retention times. For HPLC instruments, once the solute particles travel through the column they reach the detector. There are two different types of detectors; bulk property, which respond to the mobile-phase bulk property, and solute property which responds to UV absorbance, as in this current work, or fluorescence.<sup>39</sup> For solute particles to reach the detector two different properties dictate their movement. Bulk flow has to do with the potential energy gradient that causes the solution to move. In bulk flow the particles that are close to each other remain so because

of intermolecular forces. The second property that determines the flow of particles is specific motion which is just when molecules respond to a gradient of chemical and potential energy. Here, molecules respond differently so the speed of the molecules does not depend on distance nor vicinity to one another, but to the stationary and mobile phases. The mobile phase solvent if more attracted to solute particle it will help the particle move through the column faster than if it were more attracted to the stationary phase.<sup>39</sup>

In this research project, this technique is used to separate everything in solution and isolate the phosphorodithioate. HPLC is a sensitive technique and is useful in analyzing a variety of molecules, including amino acids, nucleic acids, and proteins. Though NMR can analyze these biological systems, they are typically synthesized on a smaller scale than useful for NMR. LC/MS can be used to test biological systems but phosphorodithioates are sensitive to oxidation or to the soft ionization used in electrospray, leading to the degradation of the molecule.<sup>39</sup>

### **Synthesis:**

#### **Salt bridge synthesis:**

#### **2-Bromoisophthalic acid (C):**

To a round bottom flask, potassium permanganate (1.708 g, 10.8 mmol) and a 1:1 solution of *tert*-butanol and water (8 mL) were stirred. To the stirring solution was added 2-bromo-*m*-xylene (0.72 mL, 5.4 mmol). This reaction was refluxed for three hours, and cooled to room temperature. Additional potassium permanganate (10.8 mmol) and 2 mL of 1:1 solution of *tert*-butanol and water was added to the reaction mixture, and refluxed

overnight. The hot reaction mixture was filtered through a bed of Celite and then was rinsed with water. The reaction mixture was acidified to a pH of 1 with concentrated  $\text{H}_2\text{SO}_4$  and extracted twice with ethyl acetate (50 mL). The combined organic extracts were dried over  $\text{MgSO}_4$ , filtered, and concentrated under reduced pressure to obtain the crude solid (0.257 g, 19.42 % yield)<sup>40</sup>.  $^1\text{H}$  NMR (400 MHz, *d*-methanol):  $\delta$  7.39 (t, 1H, 23.2 Hz), 7.62 (d, 2H).

#### **Dimethyl-2-bromoisophthalate (D):**

In a 25 mL round bottom, 2-Bromoisophthalic acid (0.257 g 2.05 mmol) was added to a stirring solution of methanol (2.81 mL) in 0.25 mL of 18 M  $\text{H}_2\text{SO}_4$ . The reaction mixture was refluxed at 70 °C for 18 hours and then water (1 mL) was added to the reaction mixture. The reaction mixture was neutralized with aqueous  $\text{NaHCO}_3$  and extracted with ethyl acetate (4 x 25 mL). The organic extracts were combined, dried over  $\text{MgSO}_4$ , and filtered. The filtrate was concentrated under reduced pressure to obtain the crude solid (0.138 g, 53.7 % yield)<sup>41</sup>.  $^1\text{H}$  NMR (400 MHz, *d*- $\text{CDCl}_3$ ):  $\delta$  3.94 (s, 6H), 7.50 (t, 1H, 15.6 Hz), 7.33 (d, 2H).

#### **2-Bromoisophthalic acid monomethyl ester (E):**

In a 10 mL round bottom flask, 2-bromoisophthalic acid dimethyl ester (0.138 g, 0.56 mmol) was added to a 3:1 solution of acetone: methanol (0.9 mL).  $\text{NaOH}$  (.023 g, 0.56 mmol) was added to the mixture, which was stirred for 48 hours at room temperature. The solution was concentrated under reduced pressure. The white slurry was dissolved in 1 M  $\text{NaHCO}_{3(\text{aq})}$  and extracted with ethyl acetate (3 x 15 mL). The organic layer was discarded, and the aqueous layer was acidified to pH 1 with 1 M  $\text{HCl}$ .

The aqueous layer was then extracted again with ethyl acetate (3x 15 mL). Combined organic layers were dried over  $\text{MgSO}_4$ , and filtered. The filtrate was concentrated under reduced pressure to obtain a crude solid.<sup>42</sup>

### **3-Hydroxypropanoic acid (G):**

In a 25 mL round bottom flask, 3-hydroxypropionitrile (0.95 mL, 1.406 mmol) was added to a stirring solution of NaOH (0.64 g, 16.0 mmol) in 2 mL of water. The reaction was slowly heated to 90 °C and refluxed for 8 hours, during which air was supplied in order to remove any oxygen that could react with the reactant. The reaction mixture was cooled to room temperature, acidified to a pH of 1 with concentrated HCl, and extracted with ethyl acetate (4 × 50 mL). The organic extracts were combined, dried over  $\text{MgSO}_4$ , and filtered. The filtrate was concentrated under reduced pressure to obtain the crude liquid.<sup>43</sup>  $^1\text{H NMR}$  (400 MHz, *d*- $\text{CDCl}_3$ ):  $\delta$  2.7 (t, 2.76 H, 6.4 Hz),  $\delta$  3.9 (t, 2.00 H, 15.6 Hz).

### **Benzyl 3-hydroxypropanoate (H):**

A solution of 3-hydroxypropanoic acid (0.673 g, 7.469 mmol) and  $\text{K}_2\text{CO}_3$  (1.240 g, 8.969 mmol) in anhydrous acetonitrile (13.63 mL) was slowly added to benzyl bromide (1.341 g, 7.842 mmol) in an ice water bath. The resulting mixture was stirred at room temperature for 72 hours. Water (250 mL) was added to the reaction mixture and extracted with dichloromethane (4 x 100 mL). The combined organic layers were washed successively 1 M HCl, water and a saturated solution of brine. The mixture was dried over with  $\text{MgSO}_4$ , filtered and evaporated to dryness using reduced pressure to obtain the crude liquid.<sup>44</sup>

**Synthesis of Phosphorodithioate:**

**O-((2R,3S,4S,5R)-2-((bis(4-methoxyphenyl)(phenyl)methoxy)methyl)-4-((tert-butyl)dimethylsilyl)oxy)-5-(2,4-dioxo-3,4-dihydropyrimidin-1(2H)-yl)tetrahydrofuran-3-yl) S-(2,4-dichlorobenzyl) dimethylphosphoramidothioite (K):**

A flame dried three-neck 25 mL round bottom flask was charged with 5'-O-(dimethoxytrityl)-2'-O-(tertbutyl dimethyl silyl) uridine (0.5 g, 0.76 mmol) and acetonitrile (1.9 mL) under nitrogen gas. To this stirring solution, diisopropylethyl amine (0.25 mL, 1.21 mmol) and bis(dimethylamino)chlorophosphine (0.13 mL, 0.91 mmol) were added with two syringes at the same time. This reaction mixture was stirred for thirty minutes. 2,4-dichlorobenzyl mercaptan (0.15 mL, 1.06 mmol) was added and stirred for an additional thirty minutes. The reaction was quenched with an aqueous saturated solution of NaHCO<sub>3</sub> and the product was extracted with ethyl acetate (2x25 mL). The mixture was dried over MgSO<sub>4</sub>, filtered and evaporated to dryness under reduced pressure to obtain a viscous solid. Degassed hexane was used to precipitate the crude product (0.53 g, 75.22% yield)<sup>45</sup>. <sup>1</sup>H NMR (400 MHz, *d*-CDCl<sub>3</sub>): δ 2.5 (dd, 6.29 H), 3.6 (m, 8.62 H).

**2-amino-9-((2R,3S,4S,5R)-3-((tert-butyl)dimethylsilyl)oxy)-5-(hydroxymethyl)-4-methoxytetrahydrofuran-2-yl)-1,9-dihydro-6H-purin-6-one (M):**

In a 1.5 mL microcentrifuge tube, 5'-Dimethoxytrityl-N-acetyl-Guanosine, 2'-O-acetyl-3'-succinoyl-long chain alkylamino-CPG (30.03 mg, 1 μmol) and 3 % by volume trichloroacetic acid (TCA) to dichloromethane (50 μL) and an additional amount of dichloromethane was used as the solvent (1000 μL) was added. The reaction mixture was



mixed on a Fisher Vortex Genie 2 for 15 minutes at room temperature. The trichloroacetic acid solution was removed and the solid support was rinsed with acetonitrile (4 x 1 mL).<sup>46</sup>

**O-(((2R,3S,4S,5R)-5-(2-amino-6-oxo-1,6-dihydro-9H-purin-9-yl)-4-((tert-butyl)dimethylsilyloxy)-3-methoxytetrahydrofuran-2-yl)methyl) O-((2R,3S,4S,5R)-2-(((bis(4-methoxyphenyl)(phenyl)methoxy)methyl)-4-((tert-butyl)dimethylsilyloxy)-5-(2,4-dioxo-3,4-dihydropyrimidin-1(2H)-yl)tetrahydrofuran-3-yl) S-(2,4-dichlorobenzyl) phosphorothioite (N):**

To the solid support, acetonitrile (1000  $\mu$ L), phosphorothioamidite (1.09 mg, 1.14  $\mu$ mol) and 0.45 M tetrazole solution in acetonitrile (6.7  $\mu$ L) were added. The reaction mixture was stirred at room temperature for 10 minutes for the first trial and thirty minutes for the second trial of this synthesis. Tetrazole mixture was removed and the solid support was rinsed with acetonitrile (4 x 1 mL).<sup>47</sup>

**(2R,3S,4S,5R)-4-acetoxy-5-(2-amino-6-oxo-1,6-dihydro-9H-purin-9-yl)-2-((((((2R,3S,4S,5R)-5-(2-amino-6-oxo-1,6-dihydro-9H-purin-9-yl)-2-(((bis(4-methoxyphenyl)(phenyl)methoxy)methyl)-4-((tert-butyl)dimethylsilyloxy)tetrahydrofuran-3-yl)oxy)((2,4-dichlorobenzyl)thio)phosphorothioyl)oxy)methyl)tetrahydrofuran-3-yl 4-amino-4-oxobutanoate (O):**

To the solid support, acetonitrile (1000  $\mu$ L) and 0.5 M (*E*)-5-(2-(dimethylamino)vinyl)-3*H*-1,2,4-dithiazole-3-thione (DDTT) in 40 % pyridine and 60% acetonitrile (24  $\mu$ L) were added. The reaction mixture was stirred for 20 minutes during

the first trial and 40 minutes for the second trial. The DDTT mixture was removed and the solid support was rinsed with acetonitrile (4 x 1 mL).<sup>45</sup>

**(2R,3S,4S,5R)-4-acetoxy-5-(2-amino-6-oxo-1,6-dihydro-9H-purin-9-yl)-2-((((((2R,3S,4S,5R)-5-(2-amino-6-oxo-1,6-dihydro-9H-purin-9-yl)-2-((bis(4-methoxyphenyl)(phenyl)methoxy)methyl)-4-((tert-butyl)dimethylsilyl)oxy)tetrahydrofuran-3-yl)oxy)(mercapto)phosphorothioyl)oxy)methyl)tetrahydrofuran-3-yl 4-amino-4-oxobutanoate (P):**

To the solid support, acetonitrile (1000  $\mu$ L), thiophenol (4.89  $\mu$ L, 47.9  $\mu$ mol), triethyl amine (9.78  $\mu$ L) and 1,4-dioxane (9.78  $\mu$ L) were added. The reaction was stirred at room temperature for two hours. The thiophenolate solution was removed and the solid support was rinsed with acetonitrile (4 x 1 mL).<sup>45</sup>

**O-(((2R,3R,4S,5R)-5-(2-acetamido-6-oxo-1,6-dihydro-9H-purin-9-yl)-3,4-dihydroxytetrahydrofuran-2-yl)methyl) O-((2R,3S,4S,5R)-4-((tert-butyl)dimethylsilyl)oxy)-5-(2,4-dioxo-3,4-dihydropyrimidin-1(2H)-yl)-2-(hydroxymethyl)tetrahydrofuran-3-yl) S-hydrogen (R)-phosphorodithioate (Q):**

To the solid support a 3:1 solution of ammonium hydroxide to ethanol solution (2x1 mL) and acetonitrile (1 mL) was added. The reaction was stirred at 55 °C for two hours. The reaction was allowed to reach room temperature. The ammonium hydroxide and acetonitrile solution was removed and the solid support rinsed with a 3:1:1 solution of ethanol to acetonitrile to water (2x1 mL). The rinses were combined and evaporated to dryness using reduced pressure to obtain a white solid.<sup>45</sup>

**O-(((2R,3R,4S,5R)-5-(2-acetamido-6-oxo-1,6-dihydro-9H-purin-9-yl)-3,4-dihydroxytetrahydrofuran-2-yl)methyl) O-(((2R,3R,4S,5R)-5-(2,4-dioxo-3,4-dihydropyrimidin-1(2H)-yl)-4-hydroxy-2-(hydroxymethyl)tetrahydrofuran-3-yl) S-hydrogen (R)-phosphorodithioate (I):**

To the white solid (Q), a solution of N-methyl pyrrolidinone (135  $\mu$ L), triethyl amine (70  $\mu$ L) and triethyl amine trihydrofluoride (95  $\mu$ L) were added. The round bottom was closed with a drying tube and the reaction mixture was stirred for 1.5 hours at 65  $^{\circ}$ C. The reaction was neutralized to pH 7 and to the mixture n-butanol and water was added.<sup>45</sup>

**HPLC studies:**

Base hydrolysis experiments were conducted in order to characterize dinucleotide I. Additionally, the product mixture was run on an HPLC column (Bondclone<sup>TM</sup>, 10  $\mu$ m C18 148  $\text{Å}$ , LC Column 300 x 3.9 mm) along with two standards, guanosine and the commercially available phosphorodithioate. The mobile phase for this analysis was composed of solvent A: 0.10 M  $\text{NH}_4\text{OHAc}$  100% and solvent B: 95% ACN, 5 %  $\text{H}_2\text{O}$ . For each sample ran on the HPLC column, a gradient was used (Table 2).

Time (min.)	% B	Flow (mL/min)
0	0	1
5	0	1
25	50	1
30	50	1
40	0	1

**Table 2.** The parameters set for the samples ran on the HPLC.

**Results and Discussion:****Salt Bridge:**

The general synthetic pathway to reach desired product A is depicted in Figure 16. In order to synthesize biphenyl A, we synthesized three separate segments to eventually couple together. Molecules B, F, and I are commercially available. Compound B is oxidized to diacid C, then esterified to obtain diester methyl D and monoacidified to obtain monoacid E. Compound F is oxidized to obtain carboxylic acid G, then a benzyl protecting group is added to obtain compound H. Compounds E and H are coupled together by a base which will initiate  $S_N2$  reaction to obtain L. Compound I is reduced to the amine and converted to compound J by addition of a tert butyloxy carbonyl (Boc) protecting group. Compound J is converted to K by addition of a boronic ester. Compounds K and L are then coupled together by Suzuki Coupling<sup>48</sup> to obtain compound M. Protecting groups are then removed in order to obtain the target molecule, A.

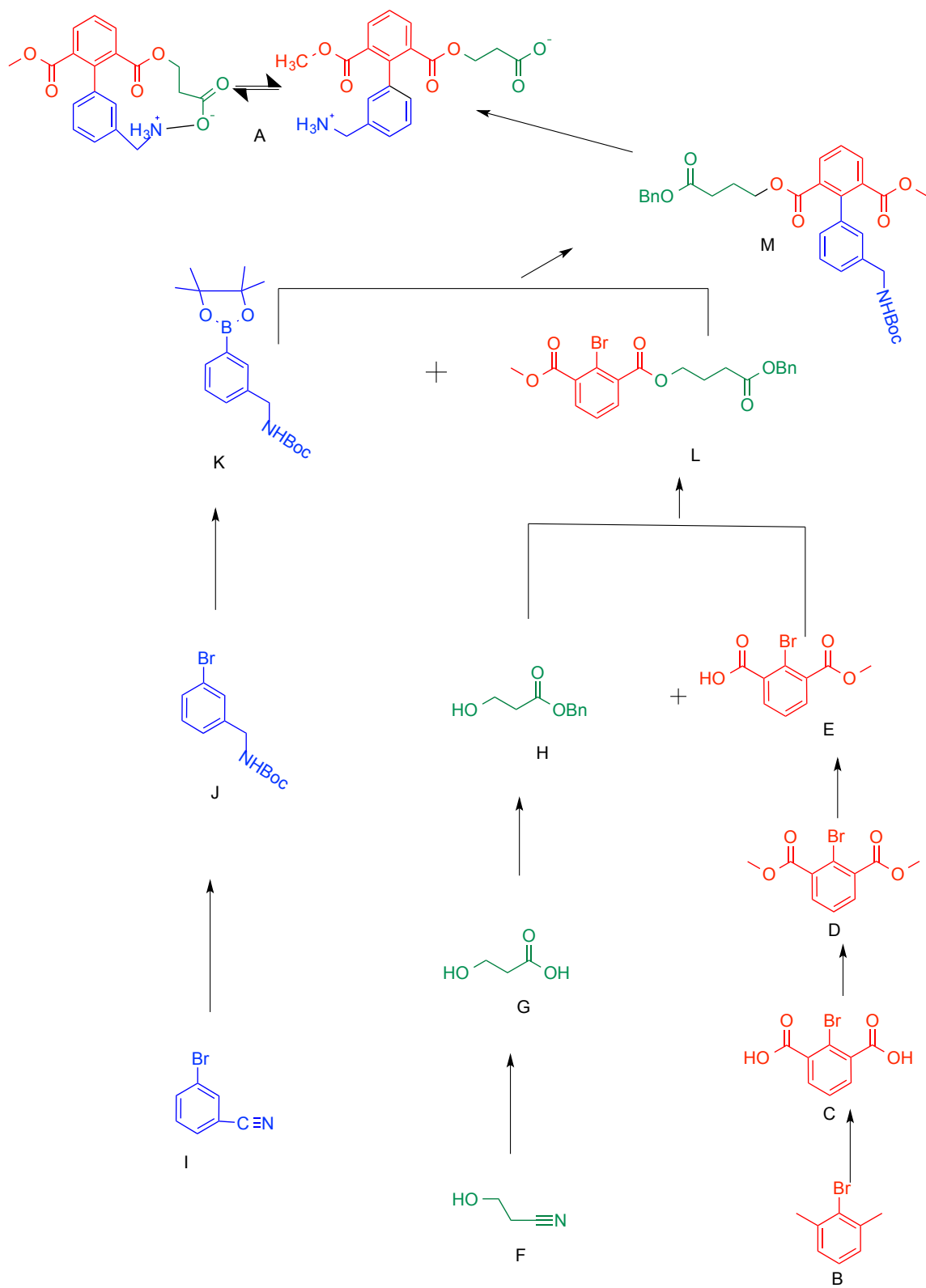
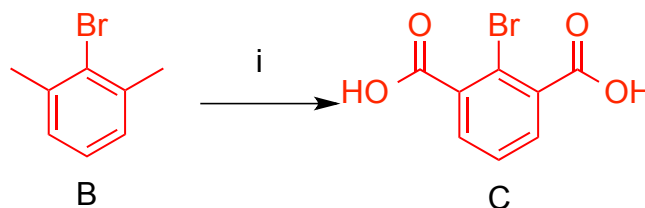


**Figure 16.** The general synthetic pathway to obtain target molecule A.



**Scheme 1.** Oxidative reaction to obtain compound C. Reagents: (i)  $\text{KMnO}_4$ ,  $\text{BuOH-H}_2\text{O}$  (1:1).

To synthesize compound C, commercially available 2-bromoxylene was successfully oxidized on a small 1.3 g scale with potassium permanganate (Scheme 1) with a 19 % yield. The crude product has a relatively simple  $^1\text{H}$  NMR (Figure 17). In addition to solvent peaks at 4.80 ppm for water and 3.21 ppm for deuterated methanol two peaks were observed, a doublet at 7.62 ppm and a triplet at 7.39 ppm assigned to peaks 2 and 3, respectively. Carboxylic acid protons show up at about 12 ppm. However, they are extremely broad and weak due to exchange of the protons for deuterium. Carboxylic acid protons were not expected to be shown in the spectrum.

The peak assignments for the  $^1\text{H}$  NMR spectrum of compound C were made based on chemical shift, integration and multiplicity. As mentioned earlier carboxylic acid protons tend to show up at around 12 ppm, but in this spectrum they were so broad as to be indistinguishable from the baseline. Compound C is symmetrical thus the protons labeled 2 are chemically equivalent and would have an integration of 2. The protons labeled 2 would be split by the proton labeled 3 and thus would have a multiplicity of a doublet, which is what is observed. Two chemically equivalent protons split the proton labeled 3 so this results in a multiplicity of a triplet and an integration of 1. The chemical shift also makes sense because protons 2 are closer to electron withdrawing groups and

thus are more deshielded. The more deshielded the protons are the more downfield, while proton 3 is more shielded and thus more upfield.

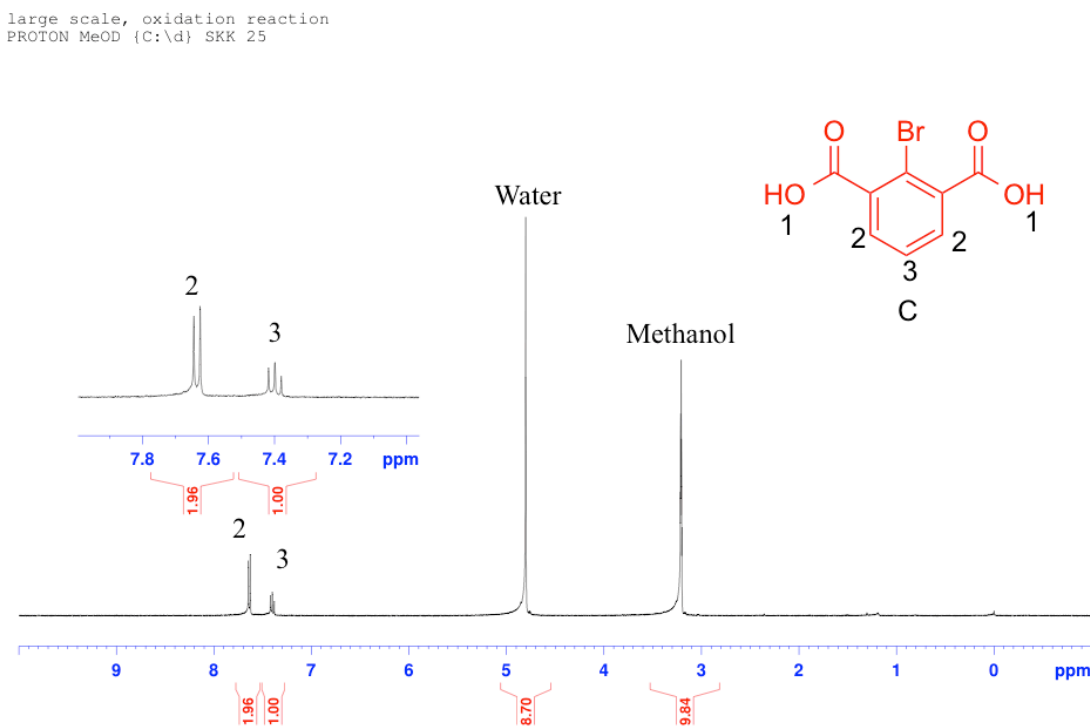
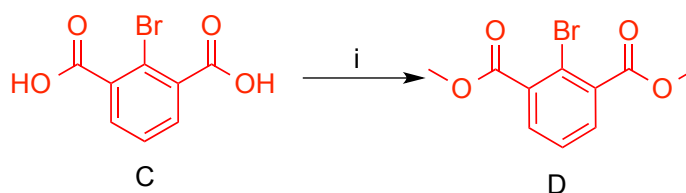


**Figure 17.**  $^1\text{H}$  NMR spectra of diacid in deuterated methanol.  $^1\text{H}$  NMR spectra displayed two peaks, a doublet and triplet, indicating isolation of pure compound C. The carboxylic acid protons were indistinguishable from the baseline.



**Scheme 2.** Diacid C is esterified to obtain compound D. Reagents: (i)  $\text{H}_2\text{SO}_4$ , MeOH.

To synthesize dimethyl-2-bromoisophthalate, compound C had to be esterified with methyl groups. Dimethyl-2-bromoisophthalate was successfully synthesized on a small 250 mg scale. Compound C was diesterified with  $\text{H}_2\text{SO}_4$  and MeOH (Scheme 2)

with 53 % yield. The crude product for this diester compound was characterized using  $^1\text{H}$  NMR (Figure 18). The spectra displayed four solvent peaks; three peaks were the extraction solvent, ethyl acetate, at 1.16 ppm, 1.9 ppm and 4.2 ppm and deuterated chloroform at 4.2 ppm. The product peaks were a singlet at 3.94 ppm for the protons labeled 1, a triplet at 7.50 ppm for proton 3, and a doublet at 7.71 ppm for the protons labeled 2.

This compound is symmetrical, so there were six chemically equivalent protons labeled 1 that were not split by anything resulting in a singlet with an integration of 6 that would show up in the alkyl region which is around 3 to 4 ppm. The protons labeled 2 had an integration of 2 and were split by the proton labeled 3 thus resulting in a doublet. The proton labeled 3 was split by two chemically equivalent protons thus resulting in a triplet with an integration of one. Chloroform appeared at 7.21 ppm and dichloromethane at 5.3 ppm.

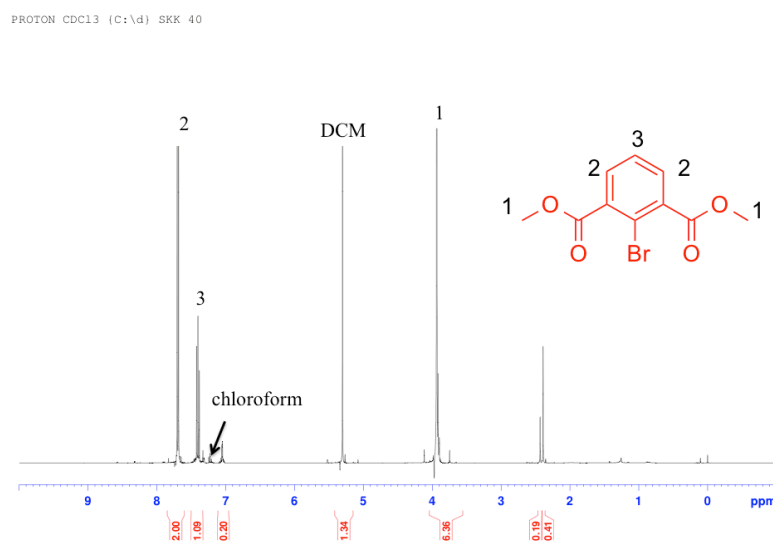
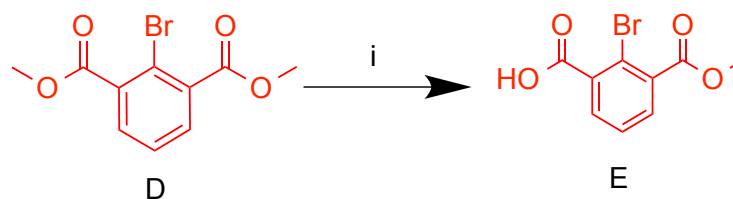


**Figure 18.**  $^1\text{H}$  NMR spectra of compound D in deuterated chloroform. The  $^1\text{H}$  NMR spectra shows all three peaks representative of compound D as well as three peaks of the extraction solvent ethyl acetate.





**Scheme 3.** Synthesis of compound E was done by a monoacidification. Reagents: (i) NaOH, Acetone:MeOH (3:1).

To synthesize compound E, a monoacidification had to be done. In the first attempt, this reaction reformed the diacid, compound C, rather than the monoacid. According to the crude product  $^1\text{H}$  NMR spectra (Figure 19), in addition to two solvent peaks, deuterated methanol at 3.32 ppm and water at 4.9 ppm, a doublet at 7.72 ppm and a triplet at 7.50 ppm were representative of the diacid forming again resulting in protons 2 and 3 being displayed.

Peaks 2 and 3 are a doublet and triplet respectively, which could be indicative of either compound E or compound C being formed. However, compound E has three protons labeled 4 that are not shown in the spectra, this means that the compound was not formed in great amounts. The ester group would show up at around 4 ppm and in that region, there is a small peak with an integration of 0.35 indicating that there was only a 10 % yield.

PROTON MeOD (C:\d) SKK 38

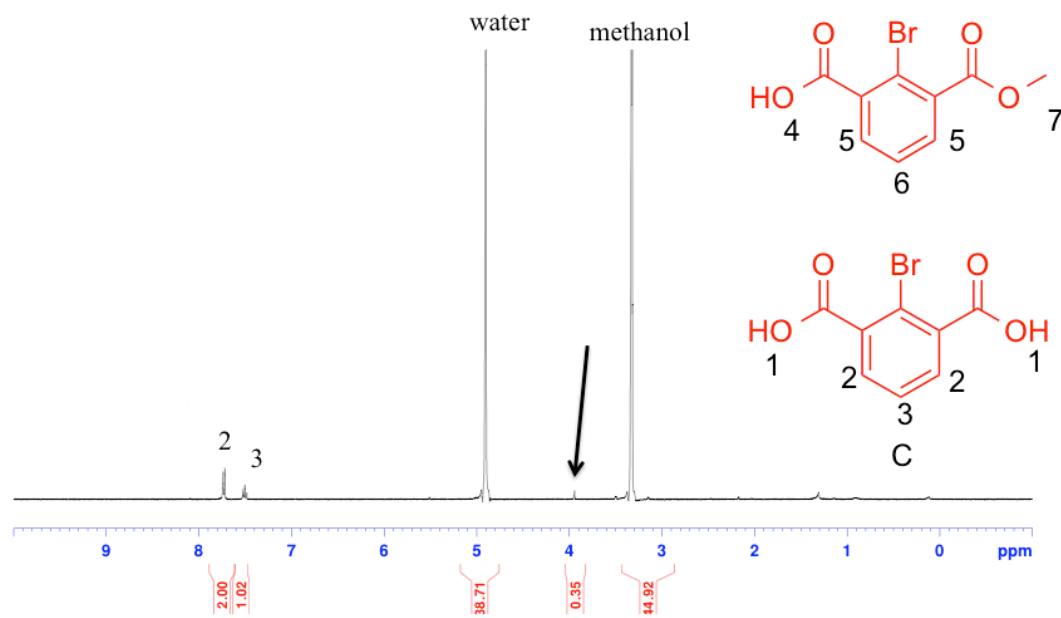


**Figure 19.**  $^1\text{H}$  NMR spectra of crude product in an attempt to synthesize compound E. This spectra showed peaks 2 and 3, but not peak 4, which indicated that compound O was not formed. Compound D was completely hydrolyzed and compound C was obtained.

In a second attempt, the reaction was monitored by TLC (Figure 20). The TLC plate had three different compounds present, the area marked A was spotted with the diacid (compound C), the region marked E with diester (compound D) and the region labeled  $\frac{1}{2}$  was the crude product mixture. The mobile phase chosen for the TLC plate was 2:1 hexanes to ethyl acetate. The mobile phase dictates what compounds run faster on the TLC plate. Since the mobile phase is more non-polar the ester would be expected to have a spot near the top, while the polarity of the diacid makes it more prone for it to remain near the baseline. The region labeled  $\frac{1}{2}$  showed some diacid and diester was present in our crude product, but it did show a new spot suggesting the monoacid may have been

successfully synthesized. The Rf value for the product was 0.103. Definitive characterization of this crude product mixture will require  $^1\text{H}$  NMR.

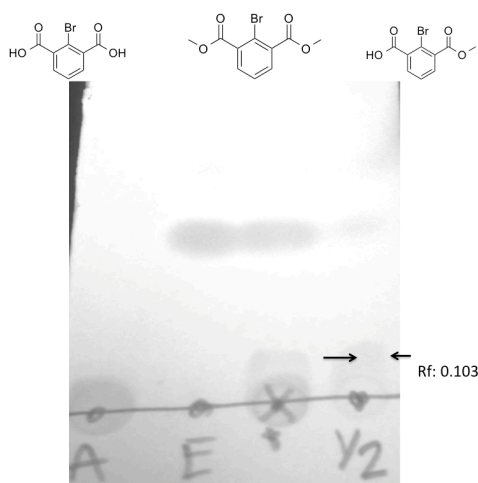
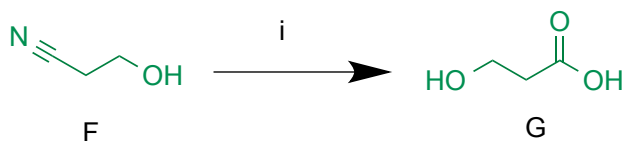


**Figure 20.** TLC plate of the crude product E. The solvent for the TLC plate was 2:1 Hexanes: Ethyl acetate. The spot marked A was spotted with diacid (B), E was spotted with diester (D), + was spotted with all components and  $\frac{1}{2}$  with crude product mixture.



**Scheme 4.** Compound F was converted to compound G under oxidative conditions. Reagents: (i) NaOH,  $\text{H}_2\text{O}$ .

In parallel, to synthesize compound G, commercially available 3-hydroxypropionitrile (compound F) was hydrolyzed with NaOH and  $\text{H}_2\text{O}$  (Scheme 4). The crude product had a  $^1\text{H}$  NMR (Figure 21), displayed many peaks indicative of different compounds present in the crude product mixture. The spectra displayed ethyl acetate at 1.10 ppm, 2.05 ppm and 4.2 ppm, as well as acetone at 2.05 ppm and chloroform at 7.2 ppm. Two methylene peaks at 2.7 and 3.7 ppm. No carboxylic acid or alcohol peak was observed for the product, although the trace vinylic peaks from 6.00 ppm to 6.56 ppm suggest a side reaction of elimination occurred. Additional peaks in the

$^1\text{H}$  NMR spectra indicated that some starting material present: 2.5 ppm, 3.99 ppm. The way the peaks of the starting material and product peaks were distinguished was by looking at the  $\Delta\delta$  in literature between protons 6 and 7 (starting material) and 2 and 3 (product). The  $\Delta\delta$  from literature was 1.27 ppm for compound G,<sup>49</sup> and 1.30 ppm for compound F.<sup>50</sup> The ratio between product and reactant was 4.8 : 2. The crude product mixture was used for the subsequent reaction. The next reaction was the addition of a benzyl protecting group to protect the alcohol of the carboxylic acid. The addition of this protecting group would not affect the starting material since no carboxylic acid is present in compound F.

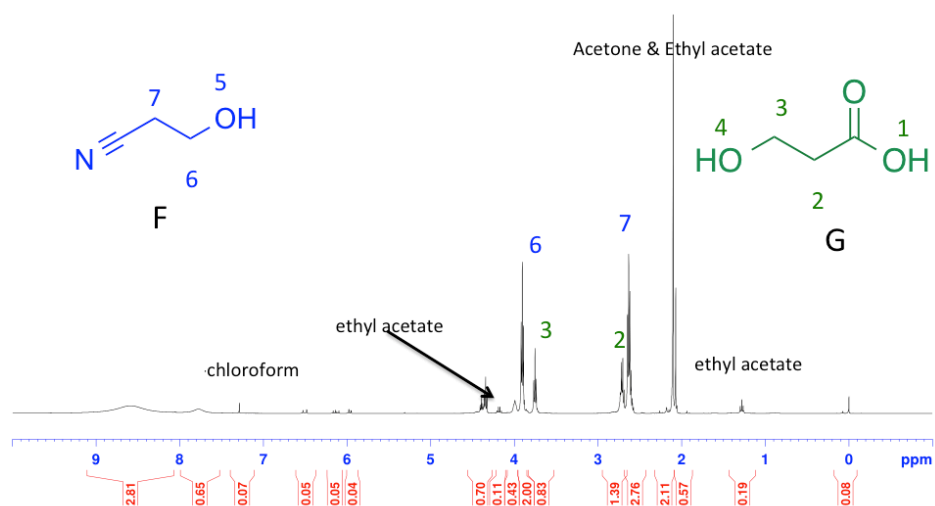
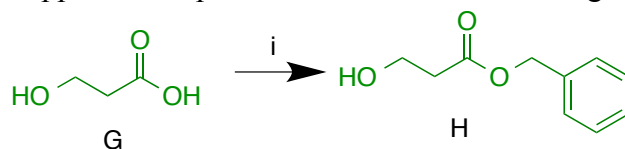


**Figure 21.**  $^1\text{H}$  NMR spectra of the crude product, compound G. Peaks 2 and 3 show that G was successfully synthesized, but no carboxylic acid peak was observed, which usually shows up at around 12 ppm. In the product there was some starting material still present.



**Scheme 5.** Compound H was generated via an  $\text{S}_{\text{N}}2$  reaction with benzyl bromide. Reagents: (i) BnBr,  $\text{K}_2\text{CO}_3$ .

Crude mixture that indicates G was used to synthesize compound H in a small 200 mg scale with benzyl bromide (BnBr) in basic conditions, potassium carbonate ( $K_2CO_3$ ) (Scheme 5). Product H and compound G could be separated by acid-base extraction. Extraction should be completed before the next step, which is a coupling reaction, since multiple products can arise if no separation is conducted. The TLC plate showed unreacted benzyl bromide in the crude reaction mixture as well as two new spots (Figure 22), which means that two new compounds were synthesized. The new spots suggest that compound H was successfully synthesized. The cross peak labeled x and P were not running evenly which could be the reason for slight change in position of each spot. Product verification should be conducted with  $^1H$  NMR. The Rf values for the two spots on the TLC plate were 0.18 or 0.30.

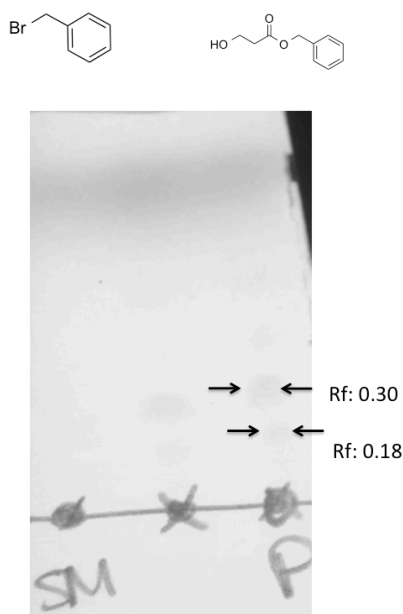


**Figure 22.** TLC plate of compound R. 2:1 Hexanes: Ethyl acetate. The spot marked SM was spotted with benzyl bromide and P was spotted with compound H. There were two new spots in the product, which indicated the synthesis of a new product, compound H.

**Phosphorodithioate:**

The general synthetic pathway to reach final product I, the phosphorodithioate dinucleotide is pictured in Figure 23. To obtain dinucleotide I, compound J must be purchased with certain protecting groups already intact, the dimethoxytrityl group and tert silyl protecting groups. Both of these protecting groups are used to protect alcohols but the reason for the different groups is to selectively remove one protecting group and not the other. The conversion of compound J to K involves the addition of a phosphine group and a benzyl mercaptan group to make a phosphorothioamidite. Then begins the one-pot solid phase synthesis. The compound is attached to a controlled pore glass bead of nucleic acid and then the solvent and reactants are added in liquid form, allowing the compound to remain on the bead while the chemistry is being done. The advantage of solid-phase synthesis is that no purification is necessary after each step, instead the removal of solvent and washing of the solid phase beads is all that is necessary. Another advantage of solid-phase synthesis is that the desired compound will remain on the bead. The disadvantage is that since it is attached to this glass porous bead it cannot be analyzed via TLC, LC/MS, or NMR because these reactions are being performed at too small (micromole) scale. Solid phase synthesis begins with compound L, which is commercially available, is selectively deprotected. Removal of the 5' dimethoxy trityl protecting group with 3 % trichloroacetic acid allows nucleophilic attack by the resulting 5'-OH. Conversion of compound N to O involves a sulfurization reaction with DDTT, subsequent compound O is converted to P by deprotection of benzyl group with thiophenol. Compound P to Q is the step where the triphenyl dimethoxy group and the

bead is removed with ammonium hydroxide to ethanol. Then removal of the silyl group with triethyl amine trihydrofluoride generates compound I.

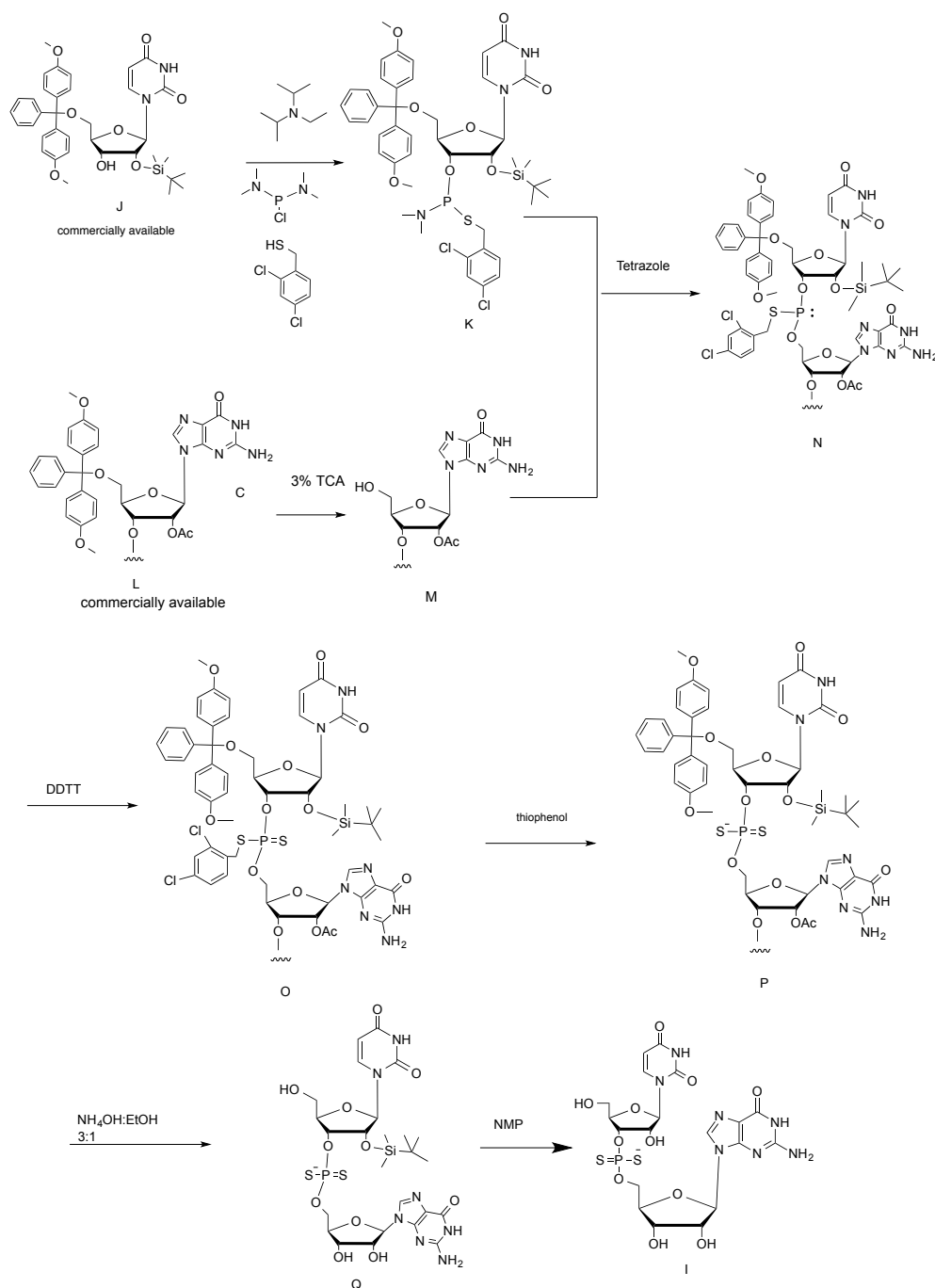
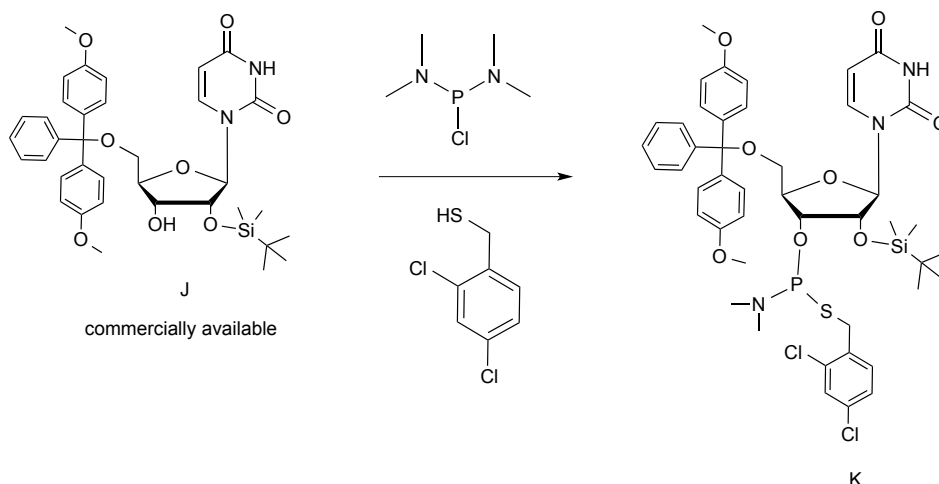


**Figure 23.** General synthetic pathway to obtain target molecule I, phosphorodithioate dinucleotide using solid phase synthesis (reagent abbreviations are given on Table of Abbreviations).



**Scheme 6.** Reagents: 1-chloro-*N,N,N,N*-tetramethylphosphanediamine, (2,4-dichlorophenyl)methanethiol triethyl amine.

Starting material J, was pure enough for use according to the  $^1\text{H}$  NMR (Figure 24a) although some small impurities may be present. Some important peaks that are representative of the compound being pure enough for synthesis of other intermediates are the protons on the amine, peak 14, which shows up as a broad singlet at around 9 ppm with an integration of 1. Also, peak 15, which overlaps with TMS, displays an integration of 6 and the splitting pattern for this peak is a singlet, but shows up as a multiplet, which indicates there may be impurities present. Peak 16 has an integration of 9 and the multiplicity is also a singlet, but shows up as a very broad multiplet. The aromatic protons are observed with the correct integration. Many peaks overlapped with each other so the splitting pattern was not as obvious in the aromatic region. Many of the peaks are broad around the top that may be attributed to impurities or to poor shimming.



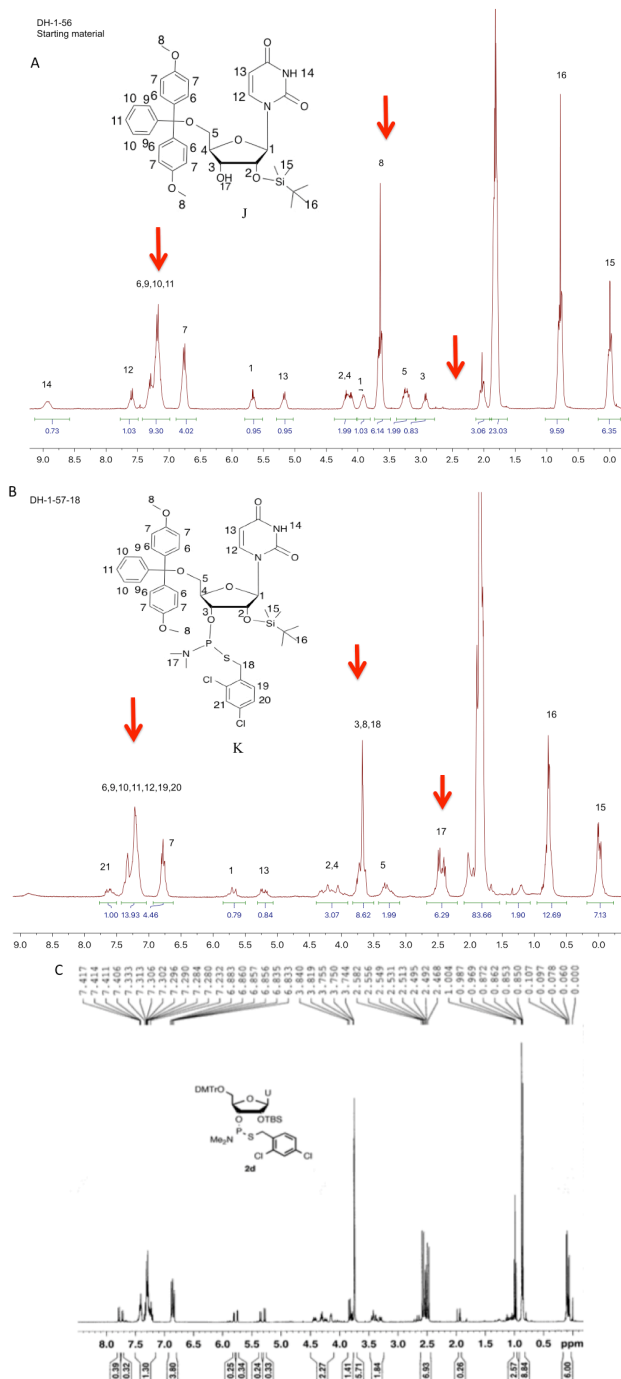


**Figure 24.** A)  $^1\text{H}$  NMR spectra of starting material J. The peaks that help identify the purity of this starting material are peaks 15, 16, 8 and 14 which all have the correct integration. B)  $^1\text{H}$  NMR spectra of crude compound K. The peaks that are representative of the successful synthesis of compound K are peaks 17, 18, and peak 21. These peaks are new peaks that did not show up in the spectra of the starting material. C) Literature  $^1\text{H}$  NMR spectra of compound K from Li et al.<sup>45</sup>

The starting material NMR spectrum was compared to the newly synthesized phosphorothioamidite K, NMR spectrum (Figure 24b). The  $^1\text{H}$  NMR of K, (Figure 24b) synthesized in the first step matches the NMR spectrum obtained from literature, Li et al. (Figure 24c).<sup>45</sup> The crude product NMR spectrum has many overlapping peaks with the starting material since no purification was done and most likely there is starting material present. Also, all of those protons on the starting material are also present on the product. The integration does correctly correspond to the total hydrogens present in the compound. There are additional aromatic peaks because an aromatic ring is added to the molecule. There is also a peak associated with the tertiary amine with methyl groups, peak 17, that has an integration of 6 and a splitting pattern of doublet of doublets since it is split by a phosphorous and the phosphorous is chiral. Also, peak 18 is observed, but it is overlapping with two other peaks.

Peak assignments for the starting material and phosphorothioamidite K were made based on ChemBio Draw results (Figure 25 & 26). In comparison with the literature  $^1\text{H}$  NMR spectrum of the phosphorothioamidite, there are many impurities. Each peak in the NMR spectrum is broader than expected due to unreacted starting material. Although only one new peak appears, peak 17, the integration does increase since many of the proton peaks overlap (Figure 24a-b).

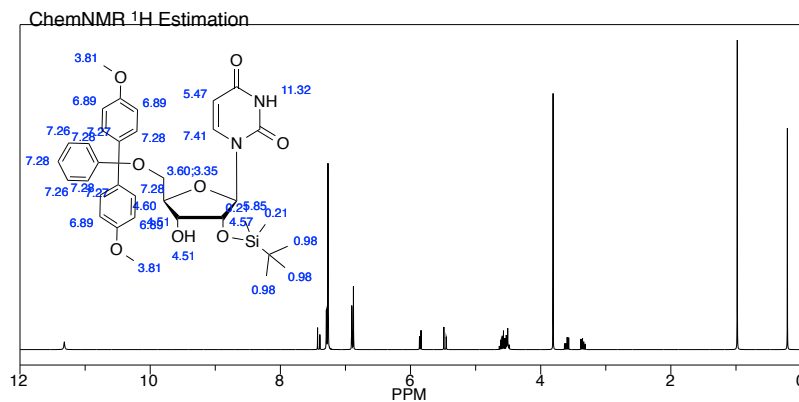


**Figure 25.** ChemBio Results  $^1\text{H}$  NMR for the starting material J.

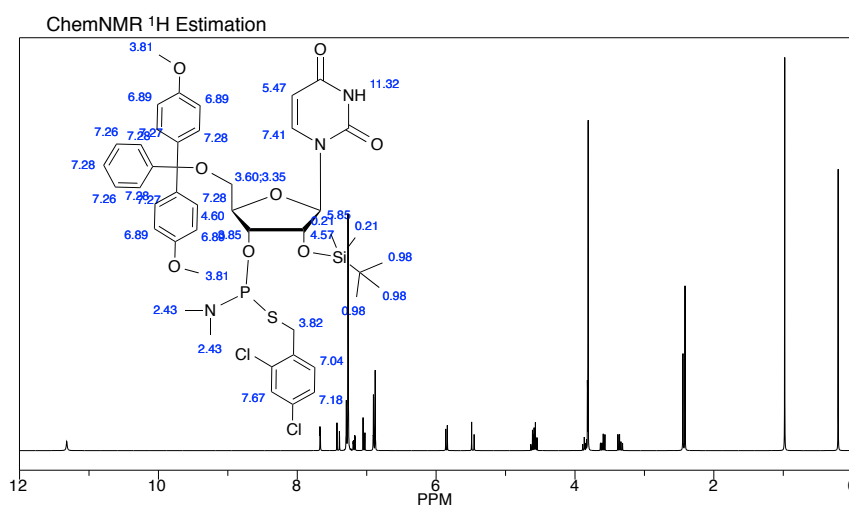


**Figure 26.** ChemBio Results  $^1\text{H}$  NMR for the phosphorothioamidite K.

Additionally, a  $^{31}\text{P}$  NMR of K (Figure 27a) was compared to the literature  $^{31}\text{P}$  NMR (Figure 27b).<sup>45</sup> There were two peaks present in both of the  $^{31}\text{P}$  NMRs due to the fact that this molecule has a chiral center with respect to the phosphorous making this compound diastereomeric. This highlights the fact that the diastereomeric forms of this compound have different chemical shifts in the  $^{31}\text{P}$  NMR. Possible impurities present in the 35 ppm region can be due to some of compound K being hydrolyzed.

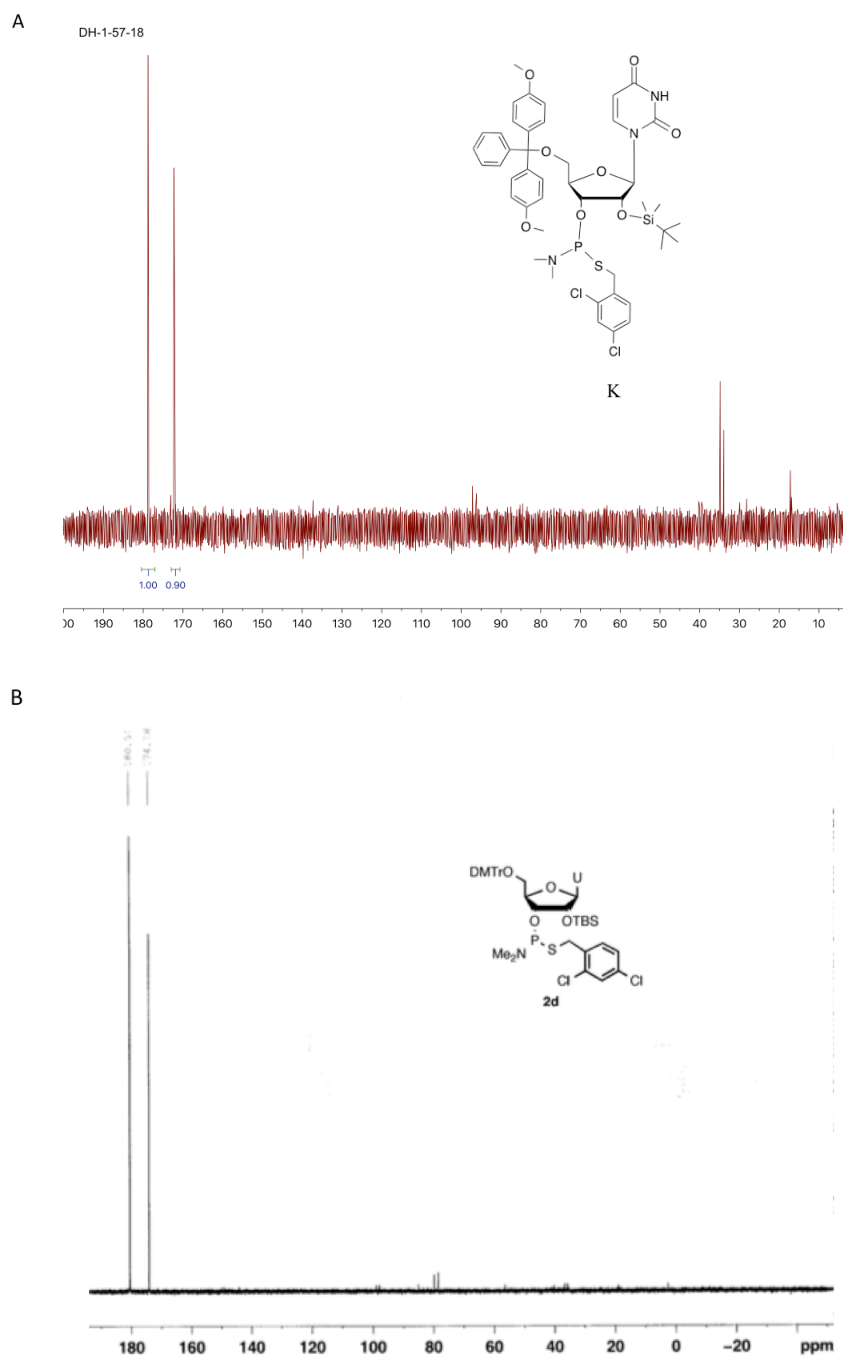


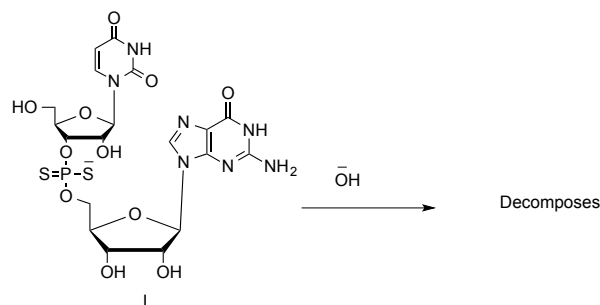
**Figure 27.** A) Phosphorous NMR of crude compound K. Two peaks are observed since this molecule is a diastereomer and one of the chiral centers is on the phosphorous. B) Literature phosphorous NMR of crude compound C from Li et al.<sup>45</sup>

Over the next 6 synthetic steps, the intermediates L through Q were not characterized. At the end of each reaction the reaction solvent surrounding the solid

support was removed and rinsed with acetonitrile. Solid phase synthesis is preferred since this makes it easier to remove any impurities. The reason why these intermediate compounds could not be characterized is because we were working at a 1- $\mu$ mol scale and so it was too small scale to characterize with NMR and also the compound was attached to a polyacrylamide bead so it could not be tested with LC/MS.

#### **HPLC studies on Phosphorodithioate:**

The chromatogram of the crude reaction mixture (Figure 28a) showed two major peaks, although other small impurities were present, at retention times of 6.661 minutes and 12.150 minutes. It was hypothesized that one of these two peaks had to be compound I. A chromatogram of guanosine was obtained (Figure 28b), in order to see if guanosine was present in our product. The retention time of guanosine in this specific mobile phase was 6.7 minutes so this indicates that one of the major peaks in the chromatogram of our crude reaction mixture was guanosine. Determination of the second major peak was attempted by a base hydrolysis experiment (Scheme 7). Base hydrolysis experiments is when base is added to reaction mixture and the mixture is analyzed in HPLC at carrying time points. In the HPLC chromatogram a decrease in the dinucleotide peak should be occurring because of phosphodiester cleavage, which would help us identify what peak is our desired product I.



**Scheme 7.** Base hydrolysis experiment done on compound I would result in its decomposition.

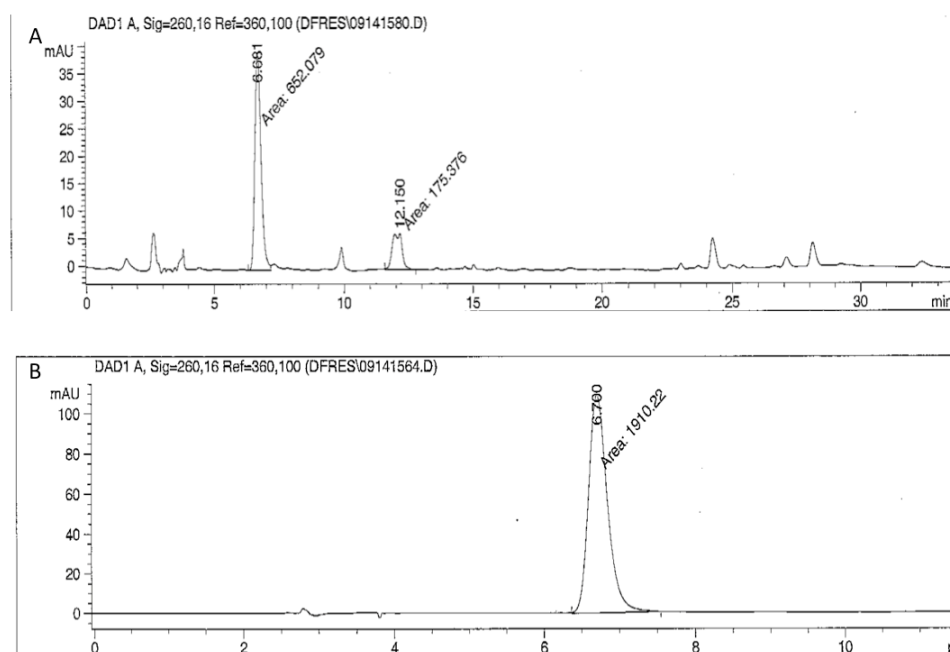


**Figure 28.** A) HPLC chromatogram of the product solution. Two major peaks are observed, one at 6.66 minutes and the other at 12.150 minutes. B) HPLC chromatogram of guanosine. The retention time of guanosine in this mobile phase was 6.7 minutes.

Base hydrolysis experiments with the obtained product mixture were conducted in an attempt to determine whether the dinucleotide was in fact synthesized. The chromatograms for the base hydrolysis experiment done on the product mixture after 30 minutes (Figure 29a) and 60 minutes (Figure 29b) show that the ratio between the two major peaks for both chromatograms was about 4; indicating that either the second major

peak is not compound I or that phosphodiester cleavage is quite slow for this compound. The peak at 12.150 minutes for thirty minutes shows a double peak, but at 60 minutes shows one of the peaks diminish. This can be indicative that the dinucleotide was synthesized, but it is not definitive.

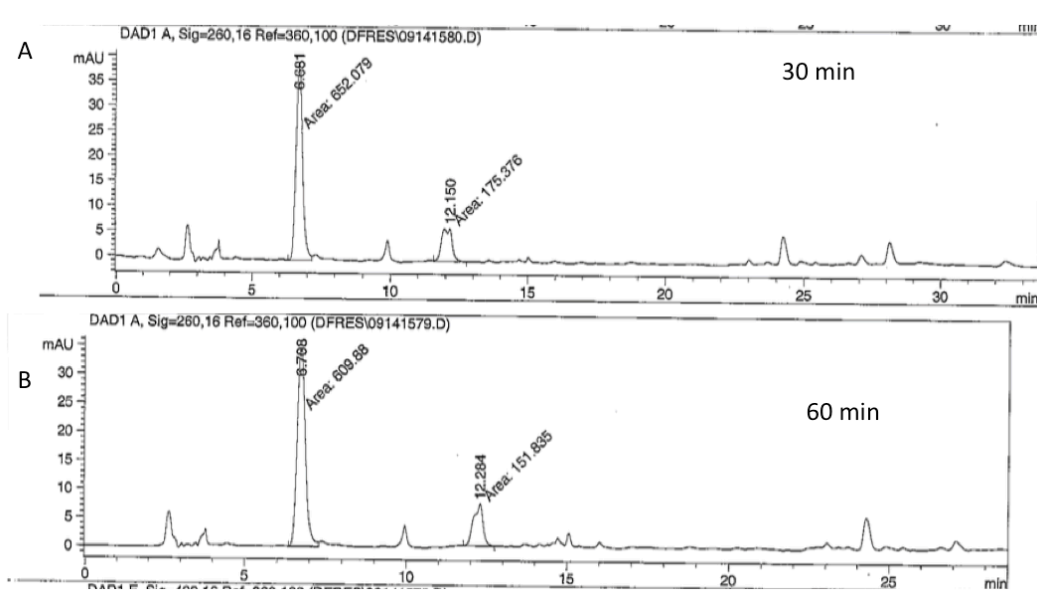
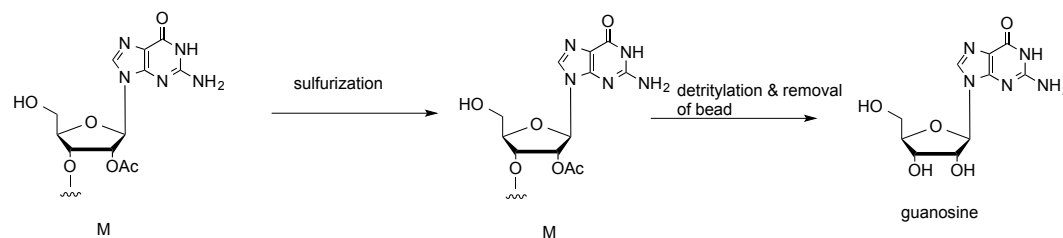


**Figure 29.** A) HPLC chromatogram of the base hydrolysis experiment done on the product solution after 30 minutes. The ratio between the two major peaks was 4. B) HPLC chromatogram of the base hydrolysis experiment done on the product solution after 60 minutes. The ratio between the two major peaks was 4.1.

The synthesis of the dinucleotide was attempted again, but with longer coupling time. The characterization with HPLC showed a large amount of guanosine, which means that the coupling reaction was not successful (Scheme 8). Longer coupling times were used for the second trial of the synthesis of the dinucleotide. Once again, characterization was again done with HPLC.



**Scheme 8.** Assuming no coupling reaction occurs, compound M is obtained, then DDTT, the sulfuration reagent is added and nothing gets sulfurized so M is still the only product and then deprotection of all the protecting groups yields guanosine.

HPLC characterization was not done by base hydrolysis studies but instead two standards were run: guanosine (Figure 30a) that had a retention time of 9.1 min and the commercially bought dinucleotide (Figure 30b), eluted at 13.4 mins. The crude product chromatogram (Figure 30c) showed no guanosine or product peak which means that one of the reactions was not successful, most likely removal of the compound from bead since guanosine was not present in the crude product solution.

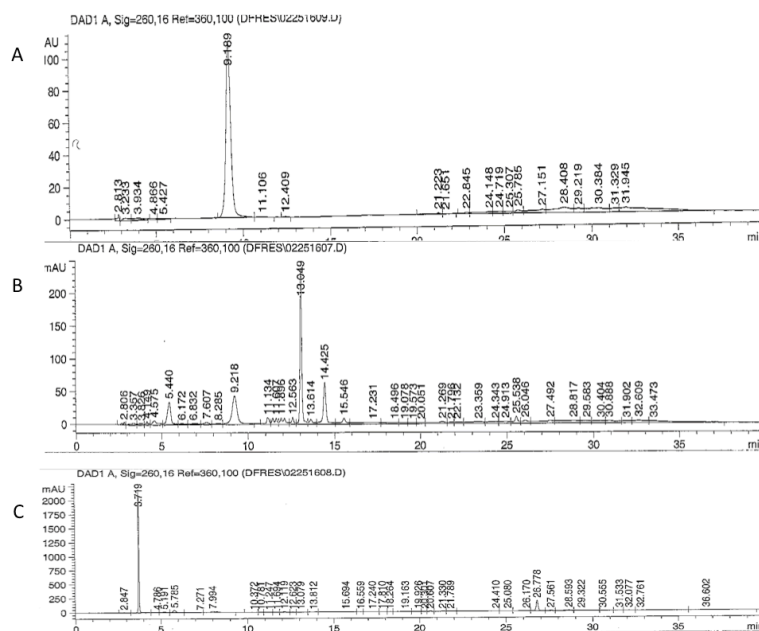


**Figure 30.** A) HPLC chromatogram of guanosine. B) HPLC chromatogram of the commercially purchased phosphorodithioate dinucleotide. C) HPLC chromatogram of the crude product mixture.



**Conclusion:****Salt Bridge:**

Surface salt bridges are especially interesting since there is great debate as to whether this interaction is a stabilizing or destabilizing force in proteins. This non-covalent interaction is present in many proteins, but no value has been associated with this interaction. Surface salt bridges are common since on the surface of the protein there are many charged residues. This interaction occurs in the presence of solvent and some speculate that the solvent may be a major factor in determining whether the salt bridge will be stabilizing or destabilizing. Some of the major factors contributing to the strength of this solvent-exposed salt bridge is desolvation, coulombic attraction, and geometric constraints. Determining the strength of this interaction can help in protein engineering to allow us to strengthen protein stability.

**Research completed/Improvements:**

Several intermediate compounds have to be synthesized in order to obtain the target molecule, A (Figure 31). Commercially available B was converted successfully to diacid C in oxidative reaction, which was then in turn diesterified to D. Commercially available F was oxidized successfully to compound G. All these compounds characterized by NMR. The synthesis of compounds E was attempted which was a monoacidification from compound D. The synthesis of compound H was also attempted, which was the addition of a benzyl-protecting group to the carboxylic acid alcohol. It is unknown whether these two compounds were successfully synthesized because

characterization was done by TLC; further characterization should be done by NMR spectroscopy.

A problem encountered during this research project was the synthesis of monoacid E. In the first attempt to obtain molecule E, the compound got fully hydrolyzed. This could be due to the fact that the scale we were working at was too small (200 mg). When working at a small scale, it is very hard for the solvent to actually cause the monoacid to crash out of solution. Since it was not precipitating, the monoacid was then further hydrolyzed to the diacid. Also, the diacid C was obtained with a poor yield, the reason why was the  $\text{MnO}_2$  was produced and it is very hard to work with. Manganese dioxide is a brown inorganic solid and when filtering it will solidify in the filter flask making the filtration process very difficult. It would be helpful to mix the solution thoroughly and continuously during the filtering process so that it does not clog the filter and discourages product loss.

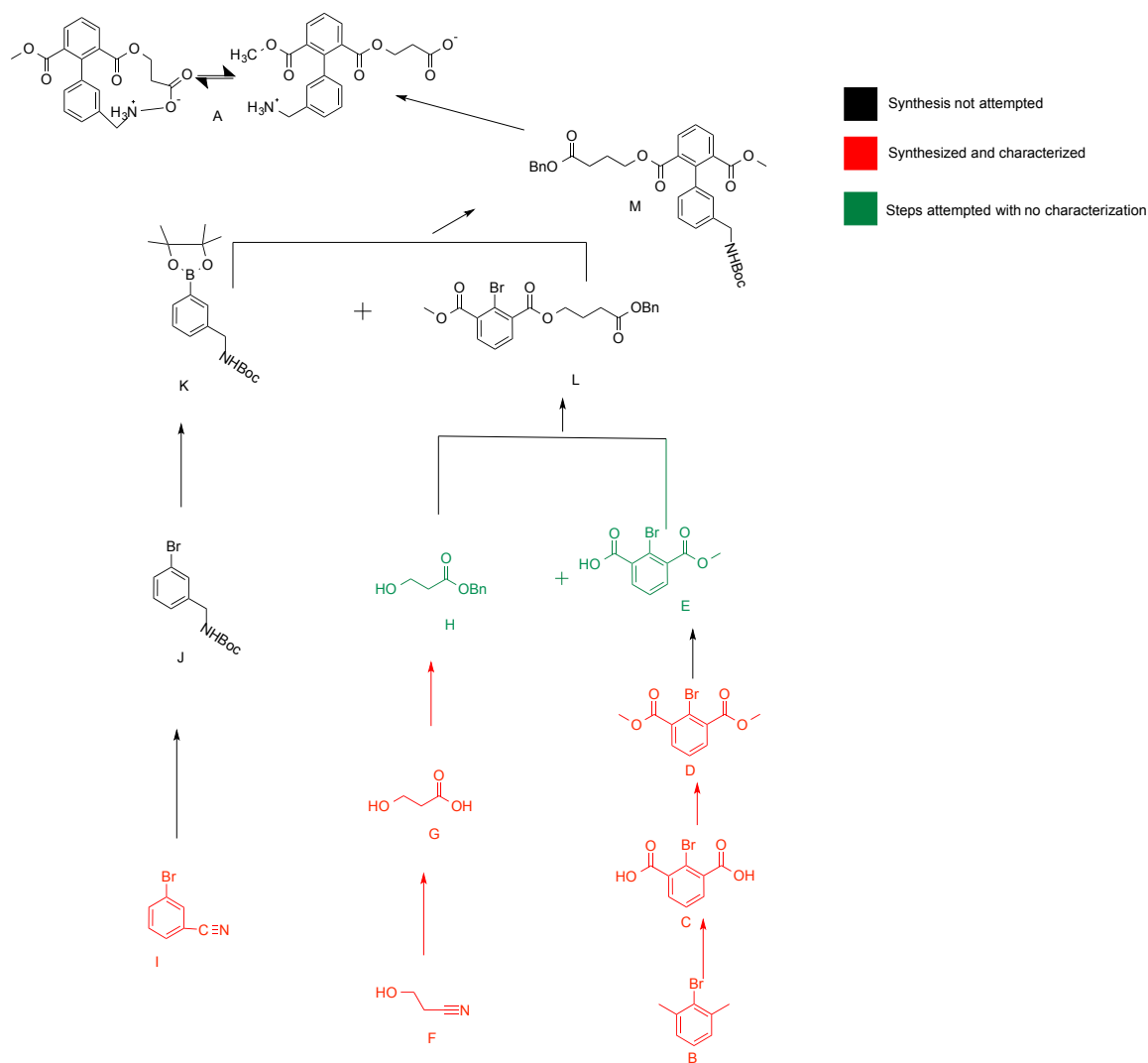


**Figure 31.** This figure highlights progress on the salt bridge project.

### Future Research:

Further research should be continued in this project. Figure 31 highlights what has been done on this project thus far. The full synthesis of this biphenyl compound should be done along with NMR characterization of all intermediate compounds. The NMR spectrum of the target molecule A will allow us to find the ratio between the two conformations of this compound, allowing us to calculate a  $K_{eq}$  value, which in turn will

allow us to calculate a  $\Delta G$  value. The  $\Delta G$  value is what governs whether an interaction is favorable or unfavorable, or in other words, stabilizing or destabilizing.

Once the small organic molecule is synthesized, a lot of studies can be done with the molecule to test the strength of the solvent-exposed salt bridge interaction. One should study this interaction in different solvents, such as protic and aprotic solvents. There should be a change in Gibbs free energy since the dielectric of the solvent is changing when you place the molecule in different solvents. The study of the biphenyl compound in varying solvents can help determine how the dielectric constant of the media affects the overall interaction. Additionally, one can study the salt bridge interaction at varying pH values, to see if a certain pH will strengthen or hinder the interaction. Lastly, the temperature that the small molecule is exposed to can allow us to see how the strength of the salt bridge interaction changes. This would be helpful in determining the major factors that make a solvent-exposed salt bridge stable or unstable. Determining the strength of solvent-exposed salt bridges can help in the area of protein engineering to make proteins more stable by altering this interaction to make it a stabilizing force.

### **Phosphorodithioate dinucleotide:**

Oligonucleotides are very important to study in order to learn about phosphodiester cleavage. Phosphodiester cleavage is the cleavage of phosphate bonds that link nucleotides together. In order for this cleavage to occur, it needs to be catalyzed by a divalent metal. In this research project we are interested in metal-ion catalyzed

phosphodiester cleavage where the hydroxyl on the 2' position is acting as the nucleophile.

The attempt to synthesize the modified dinucleotide was done so to study phosphodiester cleavage in the presence of  $\text{Ca}^{2+}$ . This metal interacts more favorably with oxygen than with sulfur so if phosphodiester cleavage in the presence of this divalent metal occurs at the same rate for dinucleotide, UpG as it does for UpS<sub>2</sub>G, then one can conclude that the mechanism for cleavage does not involve the metal interacting with the non-bridging ligands.

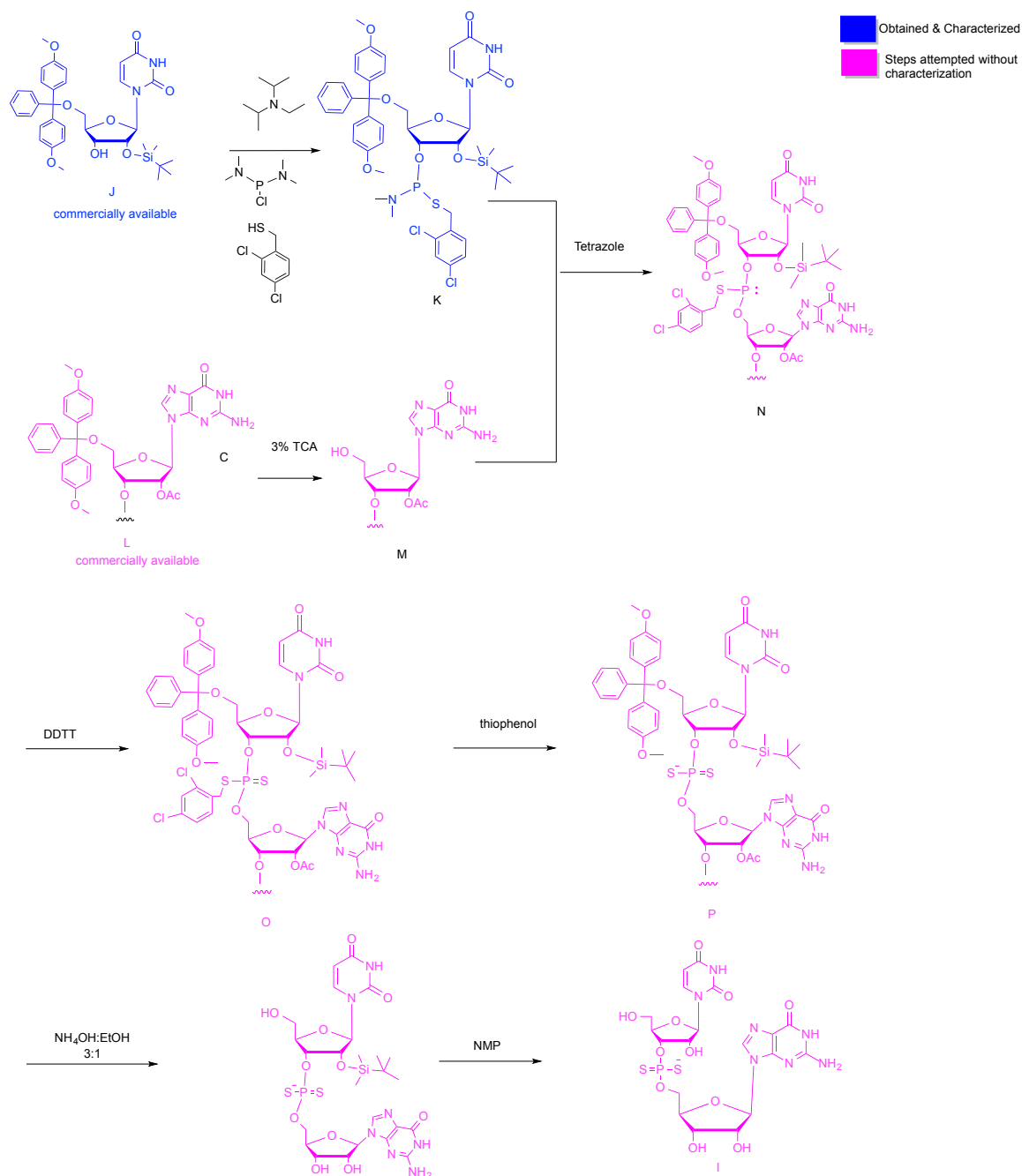


**Figure 32.** This figure highlights the progress on the phosphorodithioate synthesis project.

**Research completed/Improvements:**

The synthesis of the phosphorothioamidite K was attempted once and was successful. Characterization of this compound was done by  $^1\text{H}$  NMR and  $^{31}\text{P}$  NMR which

both matched up with NMR from literature.<sup>45</sup> Then the one-pot solid-phase synthesis was started in order to obtain dinucleotide I. Commercially available L was converted to M by removing a dimethoxy trityl protecting group with 3 % TCA. Then compound M and K were coupled together using tetrazole to obtain N. Compound N in the presence of a sulfurizing reagent yielded compound O. Thiophenol was used to remove 2,4-dichlorobenzyl group to obtain P. Then compound P was removed off the bead and the trityl protecting group was also removed using a 3:1 solution of ammonium hydroxide to ethanol. Lastly, the silyl protecting groups were removed using NMP. This one-pot synthesis was attempted twice. In the first attempt, guanosine was the major product obtained. In order to increase the yield of dinucleotide I, the synthesis was ran again with longer reaction times for certain steps, as noted in the materials and method section. The crude product obtained was analyzed by HPLC and compared to the HPLC chromatogram of the commercially available phosphorodithioate dinucleotide, but the data indicated that the dinucleotide was not successfully synthesized.

Guanosine was attained in large amounts, so longer coupling times would be helpful to ensure a larger yield of the dinucleotide. Also, since dichloromethane is used as the solvent, the amount of TCA should be changed in order to obtain 3% TCA. The bead removal and removal of dimethoxytrityl was attempted with ammonium hydroxide. The removal of the bead is generally done under basic conditions, but the removal of the dimethoxy trityl protecting group is generally done under acidic conditions. This means that removal of the trityl protecting group was not successful so an additional synthetic step should be added. Removal of the dimethoxy trityl group can be done with 3% TCA.

Lastly, this reaction sequence should be conducted at a much larger scale and removal of the bead should be done at each step. This will allow us to characterize each compound by NMR to see if each synthetic step is successful.

### **Further Research:**

The successful synthesis of the phosphorodithioate should be completed. Figure 32 highlights the progress on the phosphorodithioate synthesis project. Additional studies should be done on this compound once it is successfully synthesized. The Cassano lab should complete kinetic studies in order to determine what is the likely mechanism of metal-ion catalyzed phosphodiester cleavage. The use of different divalent metals should be reviewed in order to determine how varying the metals could affect the rate of phosphodiester cleavage. The main goal of this research project is to learn the mechanism of phosphodiester cleavage when catalyzed by divalent metal ions.

---

<sup>1</sup> Exploring biology with small organic molecules. Srockwell, B.R. *Nature*. 2004, 432, 846-854.

<sup>2</sup> Biochemistry. Berg, J., Tymoczko, J., Stryer, L. W.H. Freeman and Company. 2012, 25-33.

<sup>3</sup> Contribution of Surface Salt Bridges to Protein Stability: Guidelines for Protein Engineering. Makhatadza, G.I.; Loladze, V.V.; Ermolenko, D.N.; Chen, X.; Thomas, S.T. *J. Mol. Biol.* 2003, 327, 1135-1148.

<sup>4</sup> A Study on the Effect of Surface Lysine to Arginine Mutagenesis on Protein Stability and Structure Using Green Fluorescent Protein. Sokalingam, S.; Raghunathan, G.; Soundarajan N.P.; Lee, S. *Plos One*. 2012, 7(7), 1-12.

<sup>5</sup> Chemistry. The Molecular Science. Moore, J.W.; Stanitski, C.L.; Jurs, P.C. Cengage Learning, Inc. 2011, 402-410.

<sup>6</sup> Anticooperativity in a Glu-Lys Salt Bridge Triplet in an Isolated  $\alpha$ -Helical peptide. Iqbalsyah, T.M.; Doig, A.J. *Biochem.* 2005, 44, 10449-10456.



- 
- <sup>7</sup> Structure and dynamics of a salt bridge model system in water and DMSO. Lotze, S.; Bakker, H.J. *J. Chem. Phys.* 2015, 142, 1-9.
- <sup>8</sup> Salt Bridges Destabilize a Leucine Zipper Designed for Maximized Ion Pairing between Helices. Phelan, P.; Gorfe, A.A.; Jelesarov, I.; Marti, D.N.; Warwicker, J.; Bosshard, H.R. *Biochem.* 2002, 41, 2998-3008.
- <sup>9</sup> Electrostatic contributions to T4 Lysozyme stability: Solvent-Exposed charges versus semi-buried salt bridges. Dong, F; Zhou, H.X. *Biophys. J.* 2002, 83, 1341-1347.
- <sup>10</sup> Molecular Dynamics simulation Reveals a Surface Salt Bridge Forming a Kinetic Trap in unfolding of Truncated Staphylococcal Nuclease. Gruia, A.D.; Fischer, S.; Smith, J.C. *Proteins.* 2003, 50, 507-515.
- <sup>11</sup> Salt Bridge Energetics in Halophilic Proteins. Nayek, A.; Gupta, P.S.S.; Banerjee, S.; Mondal, B.; Bandyopadhyay, A.K. *Plos One.* 2014, 9, 1-11.
- <sup>12</sup> Protein Surface salt bridges and paths for DNA wrapping. Specker, R.M.; Record, M.J.T. *Curr. Opin. Stru. Bio.* 2002, 12, 311-319.
- <sup>13</sup> Surface salt bridges modulate DNA wrapping the Type II DNA-binding protein TF-1. Grove, A. *Biochem.* 2003, 42, 8739-8747.
- <sup>14</sup> Contribution of Salt Bridges Toward Protein Thermostability. Kumar, S.; Tsai, C.J.; Ma, B.; Nussinov, R. *J. Biomol. Struct. Dyn.* 2012, 1, 79-85.
- <sup>15</sup> Surface salt bridges modulate the DNA binding site size of bacterial histone-like HU proteins. Kamau, E.; Tsihlis, N.D.; Simmons, L.A.; Grove, A. *Biochem.* 2005, 39, 49-55.
- <sup>16</sup> Mixed-Salt effects on the conformation of a short salt-bridge-forming  $\alpha$ - helix: A simulation study. Shen, H.; Cheng, E.; Zhang, F.S. *Phys. Rev. E.* 2014, 89, 1-9.
- <sup>17</sup> Contribution of Surface Salt Bridges to Protein Stability. Strop, P.; Mayo, S.L. *Biochem.* 2000, 39, 1251-1255.
- <sup>18</sup> A Study on the Effect of Surface Lysine to Arginine Mutagenesis on Protein Stability and Structure Using Green Fluorescent Protein. Sokalingam, S.; Raghunathan, G.; Soundarajan N.P.; Lee, S. *Plos One.* 2012, 7(7), 1-12.

- 
- <sup>19</sup> Solvent-Exposed Salt Bridges Influence the Kinetics of  $\alpha$ -Helix Folding and Unfolding. Meuzelaar, H.; Tros, M.; Huerta-Viga, A.; Dijk C.N.; Vreede, J.; Woutersen, S. *J. Phys. Chem. Lett.* 2014, 5, 900–904.
- <sup>20</sup> Surface Salt Bridges, Double-Mutant Cycles, and Protein Stability: an Experimental and Computational Analysis of the Interaction of the Asp 23 Side Chain with the N-Terminus of the N-Terminal Domain of the Ribosomal Protein L9. Luisi, D.L.; Snow, C.D.; Lin, J.J.; Hendsch, Z.S.; Tidor, B.; Raleigh, D.P. *Biochem.* 2003, 42, 7050-7060.
- <sup>21</sup> Stabilization of Native and Non-native Structures by Salt Bridges in a Lattice Model of the GCN4 Leucine Dimer. Liu, Y.; Chapagain, P.P.; Gerstman, B.S. *J Phys. Chem. B.* 2010, 114, 796–803.
- <sup>22</sup> Cooperativity of complex salt bridges. Gvritishvili, A.G.; Gribenko, A.V.; Makhatadze, G.I. *Protein Sci.* 2008, 17, 1285-1290.
- <sup>23</sup> Chemical double-mutant cycles: dissecting non-covalent interactions. Cockroft, S.L.; Hunter, A.C. *Chem. Soc. Rev.* 2007, 36, 172-188.
- <sup>24</sup> Double-mutant cycles: a powerful tool for analyzing protein structure and function. Horovitz, A. *Fold Des.* 1996, 1, 121-126.
- <sup>25</sup> Altered Mechanisms of Reactions of Phosphate Esters Bridging a Dinuclear Metal Center. Humphry, T.; Forconi, M.; Williams, N.H.; Hengge, A.C. *J. Am. Chem. Soc.* 2004, 126, 11864-11869.
- <sup>26</sup> Essential Cell Biology. Alberts, Bruce et al. Garland Science. 2014, 197-258.
- <sup>27</sup> Ribozyme cleavage of a 2,5-phosphodiester linkage: Mechanism and a restricted divalent metal ion requirement. Shih, I.H.; Been, M.D. *RNA.* 1999, 5, 1140-1148.
- <sup>28</sup> An Overview of Chemical Processes That Damage Cellular DNA: Spontaneous Hydrolysis, Alkylation, and Reactions with radicals. Gates, K.S. *Chem Res Toxicol.* 2009, 22, 1747-1760.
- <sup>29</sup> Phosphodiester cleavage in Ribonuclease H occurs via an associative two metal aided catalytic mechanism. Vivo, M.; Peraro, M.D.; Klein, M.L. *J.Am. Chem. Soc.* 2008, 130, 10955-10962.
- <sup>30</sup> Single substitutions of phosphorothioates in the HDV ribozyme G73 define regions necessary for optimal self-cleaving activity. Prabhu, N.S.; Dinter-Gottlieb, G.; Gottlieb, P.A. *Nucleic Acid Research.* 1997, 25, 5119-5124.

- 
- <sup>31</sup> Enhancing phosphate diester cleavage by a zinc complex through controlling Nucleophile coordination. Tirel, E.Y.; Williams, N.H. *Chem. Eur. J.* 2015, 21, 7053-7056.
- <sup>32</sup> Cleavage properties of an oligonucleotide containing a bridged internucleotide 5'-phosphorothioate RNA linkage. Kuimrlis, R.G.; McLaughlin, L.W. *Nucleic Acid Res.* 1995, 23, 4753-4760.
- <sup>33</sup> Ribonuclease P (RNase P) RNA is converted to a Cd<sup>2+</sup> ribozyme by a single Rp-phosphorothioate modification in the precursor tRNA at the RNase P cleavage site. Warnecke, J.M.; Fürste, J.P.; Hardt, W.D.; Erdmann, V.A.; Hartmann, R.K. *Proc Natl. Acad. Sci.* 1996, 93, 8924-8928.
- <sup>34</sup> Metal ion catalysis in the Tetrahymena ribozyme reaction. Piccirilli, J.A.; Vyle, J.S.; Caruthers, M.H.; Cech, T.R. *Nature.* 1993, 361, 85-88.
- <sup>35</sup> A second catalytic metal ion in a group I ribozyme. Weinstein, L.B.; Jones, B.C.N.M.; Cosstick, R.; Cech, T.R. *Nature.* 1997, 388, 805-808.
- <sup>36</sup> Identification of the Hammerhead Ribozyme Metal ion Binding site responsible for rescue of the Deleterious effect of a cleavage site phosphorothioate. Wang, S.; Karbstein, K.; Peracchi, A.; Beigwlmn, L.; Hersclag, D. *Biochem.* 1999, 38, 14363-14378.
- <sup>37</sup> Principles of Instrumental Analysis. Skoog, D.A.; Holler, F.J.; Crouch, S.R. 2007. 6<sup>th</sup> edition. Pgs. 256-276.
- <sup>38</sup> Introduction to NMR Spectroscopy. Abraham, R.J.; Fisher, J.; Loftus, P. 1988. Pgs. 1-267.
- <sup>39</sup> Principles of Instrumental Analysis. Skoog, D.A.; Holler, F.J.; Crouch, S.R. 2007. 6<sup>th</sup> edition. Pgs. 817-837.
- <sup>40</sup> Understanding Structural Isomerization during Ruthenium-Catalyzed Olefin Metathesis: A Deuterium Labeling Study. Courchay, C.F.; Sworen, J.C.; Ghiviriga, I.; Abboud, K.A.; Wagener, K.B. *Organometallics.* 2006, 25, 6074-6086.
- <sup>41</sup> Apical Functionalization of Chiral Heterohelicenes. Surampudi, S.K.; Nagarjuna, G.; Okamoto, D.; Chaudhuri, P.D.; Venkataraman, D. *J. Org. Chem.* 2012, 77, 2074-2079.
- <sup>42</sup> A Minimal Protein Folding Model to Measure Hydrophobic and CH-p Effects on Interactions between Nonpolar Surfaces in Water. Bhayana, B.; Wilcox, C.S. *Angew. Chem.* 2007, 119, 6957-6960.

- 
- <sup>43</sup>  $\beta$ -Hydroxypropionic Acid. Read, R.R. *Organic Syntheses, Coll.* 1941, 1, 321.
- <sup>44</sup> Psoromic Acid is a Selective and Covalent Rab-Prenylation Inhibitor Targeting Autoinhibited RabGGTase. Deraeve, C.; Guo, Z.; Bon, R.S.; Blankenfeldt, W.; DiLucrezia, R.; Wolf, A.; Menninger, A.; Stigter, E.A.; Wetzel, S.; Choidas, A.; Alexandrov, K.; Waldmann, H.; Goody, R.S.; Wu, Y. *J. Am. Chem. Soc.* 2012, 134, 7384–7391.
- <sup>45</sup> Automated Solid Phase synthesis of RNA oligonucleotides containing a nonbridging phosphorodithioate linkage via phosphorothioamidites. Li, N.S.; Frederiksen, J.K. Piccirilli, J.A. *J. Org. Chem.* 2012, 77, 9889-9892.
- <sup>46</sup> Efficient Activation of nucleoside phosphoramidites with 4,5-dicyanoimidazole during oligonucleotide synthesis. Vargees, C.; Carter, J.; Yegge, J.; Krivjansky S.; A.; Kropp, E.; Petersen, K.; Pieken W. *Nucleic Acids Research.* 1998, 26, 1046-1050.
- <sup>47</sup> Chemical Synthesis of dimer ribonucleotides containing internucleotidic phosphorodithioate linkages. Petersen, K.; Nielsen, J. *Tetrahedron Lett.* 1990, 31, 911-914.
- <sup>48</sup> Selection of boron reagents for Suzuki-Miyaura coupling. Lennox, A.J.J.; Lloyd-Jones, G.C. *Chem. Soc. Rev.* 2014, 43, 412-443.
- <sup>49</sup> Comprehensive NMR Analysis of Compositional Changes of Black Garlic during Thermal Processing. Liang, T.; Wei, F.; Lu, Y.; Kodani, Y.; Nakada, M.; Miyakawa, T.; Tanokura, M. *J. Agric. Food Chem.* 2015, 63, 683-691.
- <sup>50</sup> Tetrahydropyranylation of Alcohols and Phenols and their depyranylation. Chapter 3. 114-164.